nature portfolio

Peer Review File

Morphogenetic mechanical metamaterials: Emerging tensor properties from self-organized structures

Corresponding Author: Professor Thomas Fromenteze

This file contains all reviewer reports in order by version, followed by all author rebuttals in order by version.

Version 0:

Reviewer comments:

Reviewer #1

(Remarks to the Author)
The authors present a structure generation algorithm based on solving a reaction-diffusion equation to control the anisotropy of small holes, applying the methodology to the design of a perforated plate. The subsequent experimental validation demonstrating consistency between simulation and experimental results is commendable. However, despite the technical coherence of the research, the novelty, broader applicability, and transformative potential of the proposed method are not clearly articulated. Given the current scope and content, the manuscript may not meet the novelty threshold required for publication in a general-scope journal. We therefore recommend submitting this work to a specialized journal focusing on computational theory or material design.

Specific Comments for Improvement:
1. Figure 1 illustrates complex potential shape patterns, yet the manuscript strictly limits its consideration to ellipsoidal holes. Furthermore, while the concept of scalability is introduced in Figure 7, the core structure generation process does not involve changes in hole size, suggesting a strong and potentially fatal dependency on the initial conditions. This significant limitation of the proposed method requires thorough and critical discussion within the main text. If the mechanism can demonstrate that the holes can grow larger or disappear (i.e., topological changes), the claim of high scalability would be significantly strengthened.
2. To demonstrate the proposed method's broad potential, it would be beneficial to include examples of application to completely disparate material systems or structural applications.
3. Equations (4) and (5) represent fundamental principles of continuum mechanics. Such elementary equations are typically not included in the main text of a journal targeting this readership, as they are considered established background knowledge.
4. The Methods section is currently dominated by descriptions of classical mechanical content, making it difficult to discern the novel features of the authors' contribution. This section needs refinement. The authors should prioritize explaining the conceptual significance and uniqueness of the proposed work rather than detailing standard software usage procedures.
5. The distribution diagram presented in Figure 3 lacks essential context. The authors must specify what physical quantity the distribution represents and the corresponding scale. Additionally, given that shear stiffness is expected to be anisotropic, justification is required for presenting only C66. Finally, if multiple data points are displayed, the total number of calculated cases should be clearly indicated to ensure figure interpretability.
6. The authors should clarify the necessity of setting the parameter R2. Specifically, an explanation is needed regarding whether the mechanical steady state is achieved naturally by the model dynamics without explicitly prescribing R2.
7. The data presented in Figures 5 and 6 show negative displacement in the tensile direction. This outcome is unconventional and appears erroneous. The calculation methodology for displacement must be clearly explained, as the current presentation suggests a departure from common practice.
8. Since the authors are solving a design and optimization problem, the mathematical definition of the problem (i.e., the objective function, design variables, and constraints) must be explicitly stated.
9. The absence of the finite element mesh makes it difficult to ascertain the model's accuracy. Since the model is inherently 3D despite the results being presented in 2D, a visualization and description of the overall mesh resolution are crucial for validating the computational results.
10. The meaning and methodology for evaluating the homogenized elastic constants from corner-node reactions and displacements must be clearly defined and explained, as this is an unconventional approach for calculating effective material properties.

11. The periodic unit cell microstructure employed contains a notably large number of holes. The authors should justify why this high density is necessary; it is generally sufficient to use a minimal number of representative holes within the unit cell to adequately capture the effective material behavior.
12. The authors state the use of 3D EXPERIENCE for the finite element analysis. It should be explicitly confirmed whether the underlying solver used is ABAQUS Standard and the specific version number must be included for reproducibility.

(Remarks on code availability)

Reviewer #2

(Remarks to the Author)
This paper presents a morphogenesis-inspired optimization approach for designing a mechanical cloak. The authors present their simulation results along with experimental validation. They also compare their results with previously published approaches. The work is interesting and ties together optimization, simulations, and experiments. However, there are points for improvement, particularly to address the broad readership of Nature Communications.

1. The authors should consider updating the introduction to address the broad readership of Nature Communications. In particular, please provide clear definitions for the terms mechanical cloak and morphogenesis.
2. On a similar note, Figure 1 could be improved to be more illustrative of the high level concept of the paper.
2.1 Much of Figure 1 is described in the Introduction, but the figure is not referenced in the text until Results.
2.2 How was the image in Figure 1c generated?
3. The organization of the Validation section could be improved. For example, the values for Delta_hole and Delta_cloak from the simulations are not mentioned until the very end of the discussion comparing the experimental and simulation results. Please rework this section to make the comparison clearer.
3.1 It would be interesting to see the experimental and simulation results for the 3 samples compared side by side in a figure (i.e. combining Figures 5 and 6). The authors might consider adding this to either the main text or supplementary material.
4. Regarding the comparison presented in Table 1, could the authors comment on how different loading types and boundary conditions might change the calculated effectiveness of a mechanical cloak, as well as if these would affect the agreement between simulations and experiments?
4.1 The authors should consider adding an example using their system for a mechanical cloak under compression, for a more direct comparison with Ref 24.
5. Please comment further on potential applications of this work.
6. Formatting/grammar points to be addressed:
6.1 There are several typos scattered throughout the text.
6.2 Additionally, there is inconsistent capitalization and formatting of journal titles in the references.
6.3 There are a few places in the Introduction/Results sections where there are minor repeated phrases.
6.4 Equations would be better presented in the text as opposed to in figures (Figure 3d).

(Remarks on code availability)

Reviewer #3

(Remarks to the Author)
The manuscript proposes a decentralized, morphogenesis-inspired generator for mechanical metamaterials whose local effective elasticity is steered by anisotropic reaction–diffusion. A precomputed database links generative parameters to homogenized stiffness matrices. An orthotropy-preserving tensor transformation maps a cloak design into target local tensors. The nearest database entries are assigned pointwise, smoothed, snapped to realizable values and then the microstructure “self-organizes”. The approach is validated by a mechanical cloaking experiment.

The conceptual contribution is valid and results in fabricable designs, however there lacks sufficient numerical or experimental evidence that the method is robust. I suggest the following:

1. How closely do realized tensors match the targets? Can you propose an error metric (trace, anisotropy, shear and principal-direction misalignment)

2. The matching is only done using the trace and principal direction, and anisotropy and shear "follows implicitly". How would you then independently control the latter two as you state in the paper? Can you justify why this is chosen as the method.

3. Can you quantify the coverage in terms of elasticity tensor that is realizable with the method? Both in terms of how finely controllable the resulting elasticity is, and how wide the coverage is.

4. Can you discuss the possibility of multiple distinct geometries all exhibiting similar tensorial quantities? Second, will a small perturbation in lambda, sigma or theta change the geometry greatly?

5. The cloak example is only valid under uniaxial tension for one hold radius. Can you show (at least numerically) more

examples, such as shear loading, biaxial tension, or non-circular cavity?

6. Can you provide a more balanced comparison between results generated from a topology optimization type algorithm (Table 1)?

7. The 3D claim is a bit speculative, I can forsee some fundamental difficulties in extending this. Can you discuss this a bit more?

(Remarks on code availability)
NA

Version 1:

Reviewer comments:

Reviewer #1

(Remarks to the Author)
The authors have revised the manuscript in accordance with the reviewers' comments. While certain sections require further clarification, the majority of the requested revisions have been addressed, resulting in a notable improvement in the quality of the work. However, the following three points remain insufficient, and the reviewer requests that the authors address these concerns in a subsequent revision.
Specific Comments for Improvement:
5. Figure 3 Analysis: First, panels (a), (b), and (c) present deformation and distribution diagrams derived from finite element analysis; however, a legend for the distribution is missing.
Regarding panel (e), while the vertical axis (representing the trace of the stiffness matrix) is appropriate as an invariant quantity, the values on the horizontal axes appear to be coordinate-dependent. Please verify whether these values remain invariant under a coordinate system transformation. Given the material's anisotropy, the use of the Zener ratio is recommended. Regarding shear stiffness, reporting the maximum (or minimum) value would more accurately characterize the material response.
7. Figures 5 and 6: Figures 5 and 6: Since displacement measurements are inherently dependent on the choice of a reference point, it is preferable to present these results as strain to ensure objectivity and frame-indifference.
8. Optimization Formulation: A formal optimization problem must be explicitly defined for any study concerning optimal design. The authors should clearly specify the target values and the optimization problem employed to minimize the deviation from these targets.

(Remarks on code availability)

Reviewer #2

(Remarks to the Author)
The authors have submitted an extensively revised draft with significant improvements, particularly regarding the applicability to different load cases and the organization of the manuscript. However, I still have concerns to be addressed before I can recommend acceptance.

1. Figure 1 consists of two zoomed-in architecture images that are not particularly helpful or illustrative of what a mechanical cloak is, how it works, or what previous approaches have been tried. For such a broad/interdisciplinary journal, figure 1 should offer an overview of the paper's aim and general concepts, as well as illustrate any terms necessary to understand the paper (e.g. mechanical cloak). This figure still needs to be reworked and better integrated with the Introduction.

2. The rainbow color scheme used for contour plots is not accessible to color-blind readers. Please convert figures to an accessible color scheme. (Figures throughout main manuscript and supplementary material)

3. Please elaborate on the description of the microstructure as "trusses" in the caption of Supplementary Fig 12.

4. In the discussion, the authors comment that the optimization design method can be readily transferred to 3D. Please comment on the manufacturability of 3D designs.

5. In Fig 9, please clarify what the structures/insets on the right correspond to.

6. For the additional loading cases added in the revised draft, the same metrics as in Table 1 should be presented to facilitate comparison between loading cases and with previous studies.

7. The presented cloaking designs seem to have a ring of (near-) solid material around the cavity. What would be the comparison between the morphogenetic designs and a plate that just added this solid ring with no other optimization?

(Remarks on code availability)

Reviewer #3

(Remarks to the Author)
Thank you for providing additional examples of the algorithm and expanding the analysis. I recommend the paper for publication.

(Remarks on code availability)
The files can be opened (and run) using either Matlab, Abaqus and Excel.

Version 2:

Reviewer comments:

Reviewer #1

(Remarks to the Author)
The authors have adequately addressed all outstanding points from the previous round of review. The reviewer is pleased to recommend the manuscript for publication in its current form.

(Remarks on code availability)

Reviewer #2

(Remarks to the Author)
Thank you to the authors for their dedicated work on revising the manuscript.

I have one remaining note: In the caption to Figure 1, the authors state "The objective of a mechanical cloak is to protect a central region from external static loads by smoothly routing stress trajectories around it." However, in the introduction, the authors define the objective of mechanical cloaks as being to make "the displacement and stress fields outside the cloaking region remain identical to those of a homogenized medium, effectively rendering the object invisible to mechanical probing." I would agree more with the latter definition, which distinguishes a mechanical cloak from simply adding reinforcement around a void. The authors should ensure their definitions are consistent throughout the manuscript.

Otherwise, I recommend moving forward with the manuscript.

(Remarks on code availability)
No changes in this revision

Morphogenetic mechanical metamaterials

Emerging tensor properties from self-organized structures

Correspondence with the anonymous reviewers

Thomas Fromentèze,[1,2,*] **Philippe Michaud,**[3]
Ali Hassny,[4] **and Vincent Pateloup**[3]

[1] University of Limoges, CNRS, XLIM, UMR 7252, F-87000 Limoges, France

[2] Institut Universitaire de France (IUF)

[3] University of Limoges, CNRS, IRCER, UMR 7315 , F-87000 Limoges, France

[4] University of Limoges, IUT du Limousin, F-87000 Limoges, France

[*] Corresponding author: thomas.fromenteze@unilim.fr

Dear anonymous reviewers,

We thank the Editor and the Reviewers for their time and their constructive feedback. In response to their comments, we have significantly revised the manuscript and the *Supplementary Materials* to strengthen the validation, clarify the methodology, and demonstrate the broader applicability of our approach. The main modifications can be summarized as follows:

- **Robustness and Scalability Analysis:** We have expanded the validation of the method's robustness by adding statistical analysis over 10 random seeds. A scalability study comparing generation times and consistency across different domain sizes has also been added.
- **Generalization and New Applications:** We have demonstrated the method's versatility by extending the numerical validation to 6 distinct mechanical loading cases. Furthermore, we have added a new section on Stress Field Guiding (Main Text and *Supplementary Materials*), illustrating how the same morphogenetic engine can locally optimize structures for load-bearing applications (e.g., bridge, cantilever) without iterative optimization loops.
- **Error Analysis:** To address requests for more rigorous validation, we have added detailed error profiles for all tensor components (trace, anisotropy, orientation) in the *Supplementary Materials*.

- **Structural Reorganization:** In line with the reviewers' suggestions, we have streamlined the Main Text by moving standard continuum mechanics equations and technical Finite Element Analysis (FEA) details to newly created *Supplementary Materials*.
- **Clarifications:** We have provided additional details regarding the database construction and clarified the positioning of our work relative to topology optimization.

To provide a clear overview of these significant additions before diving into the detailed questions, we summarize the two major extensions: generalization across loading scenarios and stress-guided optimization in the following section.

Generalization across loading scenarios and scales

To demonstrate the robustness of our mechanical cloaking strategy, we have extended the validation from the initial tensile test to six distinct loading scenarios (tension, compression, shear, etc.). Ideally, a single generated metamaterial cloak should perform effectively regardless of the applied load. Our new extensive simulations confirm this, showing a systematic reduction in displacement error across all tested modes (Fig. 8). Furthermore, we conducted a scalability analysis by varying the growth domain size and a robustness check using 10 random seeds per case. These results confirm that the method's performance improves with resolution and remains insensitive to the stochastic nature of the generation process.

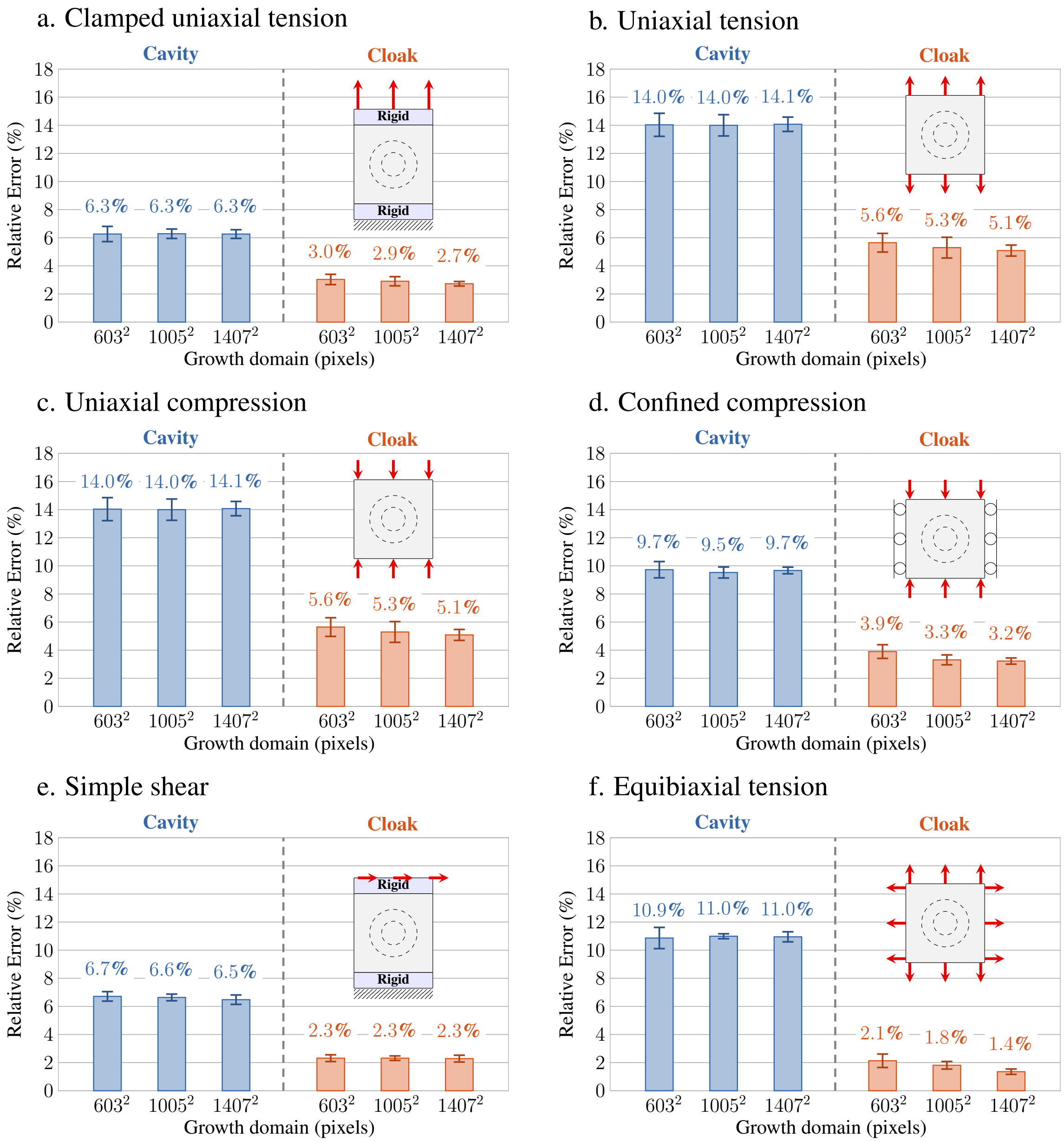

Figure C1: Summary of 6 loading modes, performed in each case for three growth domains of 603^2, 1005^2, and 1407^2 pixels and 10 random seeds. The bar plots represent the mean results obtained in each case, associated with an error bar representing a variation of $\pm$ one standard deviation. All simulations are performed by imposing displacements represented by the red arrows on each test type.

One-shot stress-guided morphogenetic growth

Addressing the query regarding potential applications beyond cloaking, we have introduced a new "one-shot" structural optimization method. By leveraging the stress field from a preliminary homogeneous simulation to drive the morphogenetic growth (adapting local density to stress magnitude and anisotropy to stress direction), we generate efficient, high-fill fraction structures in seconds. We demonstrate this capability on two structural cases: a "bridge" and a "cantilever" (Fig. 9 from main article). In both instances, the morphogenetic structures achieve significant energy reduction compared to uniform benchmarks, without relying on computationally expensive iterative optimization loops.

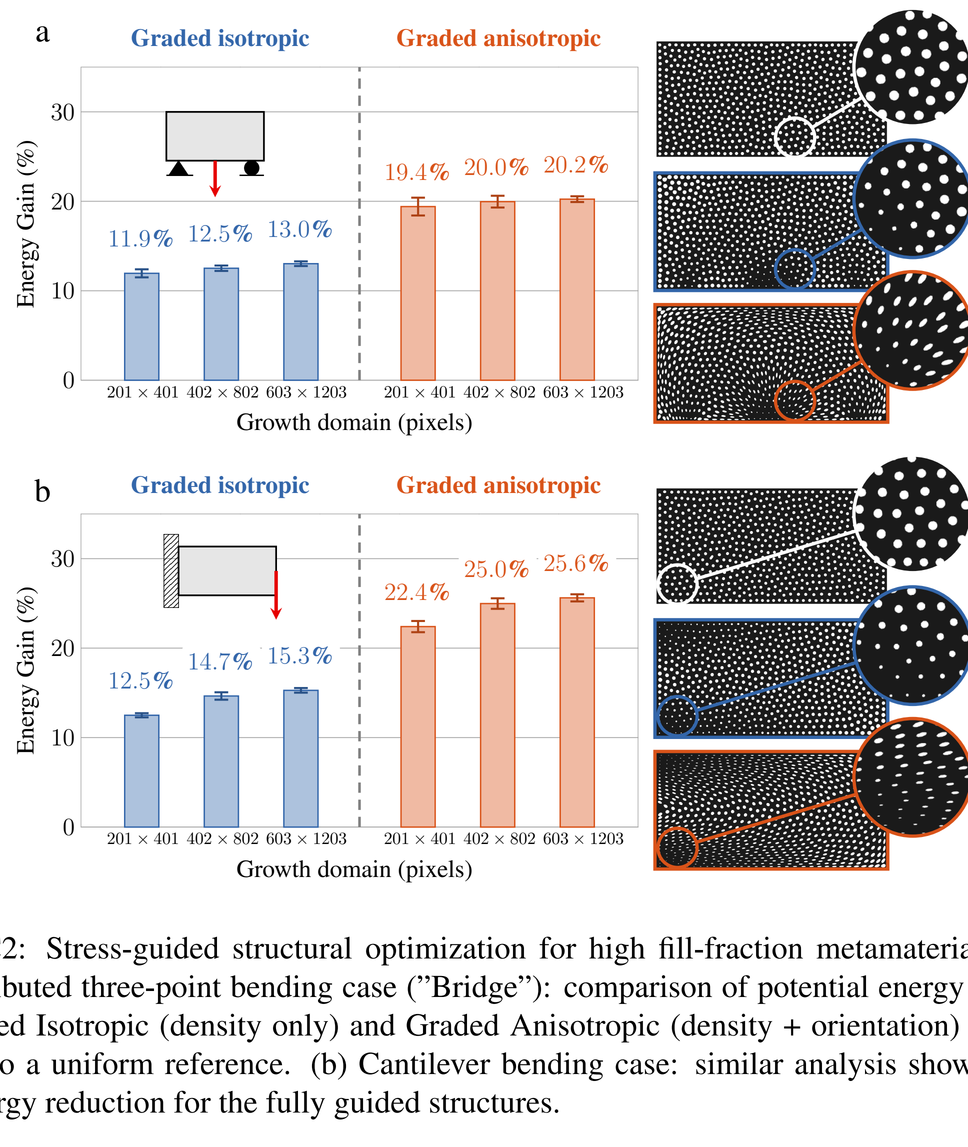

Figure C2: Stress-guided structural optimization for high fill-fraction metamaterials (80%). (a) Distributed three-point bending case ("Bridge"): comparison of potential energy reduction for Graded Isotropic (density only) and Graded Anisotropic (density + orientation) structures relative to a uniform reference. (b) Cantilever bending case: similar analysis showing up to 25% energy reduction for the fully guided structures.

1 Reviewer #1

The authors present a structure generation algorithm based on solving a reaction-diffusion equation to control the anisotropy of small holes, applying the methodology to the design of a perforated plate. The subsequent experimental validation demonstrating consistency between simulation and experimental results is commendable. However, despite the technical coherence of the research, the novelty, broader applicability, and transformative potential of the proposed method are not clearly articulated. Given the current scope and content, the manuscript may not meet the novelty threshold required for publication in a general-scope journal. We therefore recommend submitting this work to a specialized journal focusing on computational theory or material design.

We appreciate the detailed analysis of our manuscript and the constructive comments. In this response, we clarify the points raised to demonstrate the relevance of our work for publication in Nature Communications.

We are convinced that the conceptual shift brought by our approach, which enables the decentralized generation of mechanical structures inspired by morphogenesis, represents a significant advance in the field of metamaterials. This shift rests primarily on the strategy of decentralizing the structure generation process, which offers favorable scalability properties compared to classical centralized methods such as topology optimization. In light of your comments, we have strengthened the discussion around these aspects in the revised manuscript, highlighting the unique advantages of our method compared to existing approaches.

We also hope that clarifying the specific points you raised will help demonstrate the value and relevance of our work for a broader readership. We have taken care to respond to each comment in detail below, emphasizing the modifications made to the manuscript to improve its clarity and impact.

Modifications made to the manuscript are indicated at the end of each response and will be highlighted in blue in the revised manuscript.

Specific Comments for Improvement:

1. Figure 1 illustrates complex potential shape patterns, yet the manuscript strictly limits its consideration to ellipsoidal holes. Furthermore, while the concept of scalability is introduced in Figure 7, the core structure generation process does not involve changes in hole size, suggesting a strong and potentially fatal dependency on the initial conditions. This significant limitation of the proposed method requires thorough and critical discussion within the main text. ***If the mechanism can demonstrate that the holes can grow larger or disappear (i.e., topological changes), the claim of high scalability would be significantly strengthened.***

We appreciate this comment, which highlights the need to clarify several key aspects of our approach. This question raises four distinct issues that we address separately: the choice of elliptical patterns and positioning relative to existing approaches, the multi-scale control capabilities of the generative model, the robustness to initial conditions, and the topological emergence in our structures, corresponding to an actual key advantage of the proposed work.

How does our approach position itself relative to existing approaches and why choose elliptical patterns?

The structures shown in Fig. 1a and 1b correspond to existing solutions from the literature, relative to which we position our contribution. These approaches present complementary limitations that motivate our choice of elliptical patterns.

Pentamode structures (Fig. 1a) enable control of locally synthesized tensors over a wide range of values and effective decoupling of shear and bulk modes to facilitate implementation of transformation methods. However, this decoupling induces strong stress concentrations on connecting elements that must be made thin, potentially leading to structural failure under realistic loading conditions. Solutions based on pixelated periodic cells (Fig. 1b), assimilated to orthotropic tensors, offer flexibility in database construction. These patterns are characterized with periodic boundary conditions, which can be strongly impacted by sudden variations in geometry and topology of neighboring elements once implemented in structures. These effects can be exacerbated by the existence of discontinuities between cells, as illustrated in this case.

Our approach based on self-organized elliptical patterns offers a compromise. The patterns are characterized under periodic boundary conditions similar to pixelated approaches, but the self-structuring capability ensures more regular spacing between elements despite local variations in orientation and anisotropy. This property mitigates the geometric discontinuity issues observed in conventional periodic approaches while avoiding the structural fragility of pentamode structures.

Does the method allow for multi-scale control and hole size variation?

The generative model offers the possibility to control the shape of generated patterns through diffusion coefficients, directly impacting the spatial frequencies of emerging patterns through instability and bifurcation phenomena. To support this claim, we now provide several examples of multi-scale generations, and this assertion is accompanied by the addition of a mathematical development presenting the link between diffusion coefficients and spatial frequency in the *Supplementary Materials*.

Is the method robust to initial conditions?

Beyond local control of elliptical hole size made possible with our method, you mentioned a concern about robustness to initialization conditions. This point represents in our view one of the main advantages of the proposed generation method, and this comment highlights an evident need to make this property much more obvious to readers with statistical studies, now included in the revised article.

Our generative model enables self-organized emergence of structures free from uniformity constraints. This characteristic implies that we actually have the possibility to synthesize an infinite number of structures by modifying initial conditions, which will converge toward the same properties once growth is complete, despite different internal pore distributions.

These properties are related to the theme of partially correlated hyperuniform materials. The absence of symmetry in the meta-atom distribution allows obtaining great robustness to manufacturing defects. Our recent work has demonstrated that introducing controlled disorder into periodic arrangements can improve electromagnetic performance by reducing sensitivity to fabrication variability:

- Chehami, F., Decroze, C., Pasquet, T., Perrin, E., & Fromenteze, T. (2023). Morphogenetic design of self-organized correlated disordered electromagnetic media. ACS photonics, 10(6), 1890-1898.
- Fromenteze, T., Yurduseven, O., Uche, C., Arnaud, E., Smith, D. R., & Decroze, C. (2023). Morphogenetic metasurfaces: unlocking the potential of turing patterns. Nature Communications, 14(1), 6249.
- Uche, C. N., Parsaei, N., Decroze, C., & Fromenteze, T. (2025). Breaking Periodicity with Morphogenetic Metasurfaces. IEEE Transactions on Antennas and Propagation.

To demonstrate this robustness in a mechanical context, we compare performance from a series of 10 complete structures, realized from 10 different random seeds, for each mechanical loading scenario. The metric used quantifies the variation of displacement fields between different realizations, showing weak dependence on random pore positions despite different internal microstructure distributions.

Can the method handle topological changes?

The proposed generative model **precisely enables topological changes**. These properties are ensured by the self-replication capability of elliptical patterns, present until filling of available space and under constraints of local generative parameters for size, anisotropy, and orientation controls.

Pore number reduction is also present through two mechanisms. First, local pore disappearances under pressure from neighboring elements occur, though these phenomena are rare since growth is efficient and progressively fills available space, ensuring new duplications only when space is available and generated by pressure from neighboring cells. More evident pore closures occur through binary segmentation, as realized at the cloak center to increase rigidity up to the maximum value offered by the solid plate.

Modifications made to the manuscript:

- **Robustness analysis:** We have provided a synthetic overview in the Main Text (Section ”Generalization across loading scenarios and scales”, Fig. 8), while a detailed statistical analysis evaluating performance across 10 random seeds for 6 different loading cases is available in the *Supplementary Materials* (Section ”Analysis of six loading cases with the mechanical cloak”).
- **Scalability demonstration:** We demonstrated the method’s scalability in the Main Text (Fig. 7) with generation time metrics. The impact of scalability on cloaking performance is detailed in the *Supplementary Materials* (Section ”Analysis of six loading cases with the mechanical cloak”).
- **Topological adaptation:** We clarified in the Main Text (Section ”Generalization across loading scenarios and scales”) how the reaction-diffusion dynamics ensure self-organization and seamless adaptation to domain size, managing local pore distribution without mesh dependency.

2. To demonstrate the proposed method’s broad potential, it would be beneficial to include examples of application to completely disparate material systems or structural applications.

Demonstrating the broader applicability of our morphogenetic approach is indeed essential to establish its transformative potential. To address this, we have expanded our study in two directions: generalizing the mechanical cloak to diverse loading conditions and extending the method to structural optimization for specific load cases.

Can the cloaking method be extended to different loading modes?

To demonstrate the robustness of our approach, we have extended the numerical validation of the mechanical cloak to six distinct loading scenarios: clamped calibration (experimental case), standard uniaxial tension, uniaxial compression, confined compression, simple shear, and equibiaxial tension. These results, detailed in the newly constituted *Supplementary Materials*, confirm the stability of the method across diverse boundary conditions. This extension also facilitates comparison with existing literature, particularly studies focusing on compressive or shear regimes. However, it is important to note that quantitative performance metrics (such as the improvement factor defined on displacement fields) exhibit a strong dependence on specific boundary conditions (anchoring, free surfaces) and the ”padding” between the cloak and the boundaries. Consequently, while these results demonstrate the intrinsic versatility of the generated material, direct quantitative comparisons between different setups remain weakly representative.

Can the method be applied to optimize structures for specific loading types?

Beyond the general problem of cloaking, we investigated whether the morphogenetic growth could be tailored to optimize structures for specific, non-trivial loading cases. We implemented a ”stress-guided” growth strategy where the local anisotropy and orientation of the material self-organize according to the principal stress trajectories of a reference homogeneous structure. We validated this approach on two standard structural engineering cases: a distributed three-point bending problem (”Bridge”) and a cantilever beam. In both cases, the morphogenetic process spontaneously generated optimized, truss-like microstructures aligned with the load paths, significantly reducing the strain energy compared to isotropic benchmarks. These examples, detailed in the *Supplementary Materials* and the new ”One-shot stress-guided morphogenetic growth” section of the Main Text, demonstrate the potential of the method for rapid, decentralized structural optimization.

Modifications made to the manuscript:

- **Reciprocity validation:** We added a new section in *Supplementary Materials* verifying the equivalence of tensor databases constructed under tension and compression (Section ”Equivalence of Tension and Compression Databases”, Fig. 20–21).
- **Generalization:** We included 6 loading scenarios of the mechanical cloaking application.
- **Stress field guiding:** We added a new synthetic section ”One-shot stress-guided morphogenetic growth” in the Main Text, while extensive implementation details and results for the Bridge and Cantilever cases are provided in the *Supplementary Materials* (Section ”Analysis of Stress-Field Guided Growth”).

3. Equations (4) and (5) represent fundamental principles of continuum mechanics. Such elementary equations are typically not included in the main text of a journal targeting this readership, as they are considered established background knowledge.

We acknowledge this comment and agree that these fundamental equations may be too elementary for the main text. In the initial version of our article, we included them to provide a self-contained presentation that ensures clarity for readers from diverse backgrounds, given the interdisciplinary nature of Nature Communications. To propose a more concise article, we have restructured the paper and moved the most elementary parts to newly created *Supplementary Materials*.

Modifications made to the manuscript:

- **Equation streamlining:** Migration of elementary continuum mechanics equations to the *Supplementary Materials* (Section "Tensor Formalism in Mandel-Kelvin Notation").

4. The Methods section is currently dominated by descriptions of classical mechanical content, making it difficult to discern the novel features of the authors' contribution. This section needs refinement. The authors should prioritize explaining the conceptual significance and uniqueness of the proposed work rather than detailing standard software usage procedures.

In light of this comment and in relation to the previous question, we have rebalanced the writing to better highlight our contribution. We have significantly shortened the descriptions of standard mechanical steps and moved technical details (such as mesh generation and specific software usage) to the *Supplementary Materials*. The revised *Methods* section now focuses primarily on the reaction-diffusion generative model, the database construction pipeline, and the synthesis algorithm, which constitute the core novelty of our work.

Modifications made to the manuscript:

- **Content focus:** The *Methods* section has been rewritten to focus primarily on the reaction-diffusion generative model and the specific synthesis pipeline.
- **Supplementary detail:** Technical details regarding the standard finite element implementation and software usage have been moved to a dedicated section in the *Supplementary Materials*.

5. The distribution diagram presented in Figure 3 lacks essential context. The authors must specify what physical quantity the distribution represents and the corresponding scale. Additionally, given that shear stiffness is expected to be anisotropic, justification is required for presenting only C66. Finally, if multiple data points are displayed, the total number of calculated cases should be clearly indicated to ensure figure interpretability.

The reviewer correctly identifies that Figure 3 requires clarification. This comment raises three distinct points that require clarification regarding our database construction: the physical meaning and units of the plotted distributions, the representation of shear stiffness through the single component C66 in an orthotropic framework, and the quantification of the database size.

What are the physical quantity, scale, and units of the distribution?

Figures 3a, b, and c are indeed presented in a qualitative role, representing the procedure used to determine the different coefficients of the elasticity tensor. These successive simulations are performed by generating periodic supercells and implementing simulations with periodic boundary conditions. The quantities represented in these three figures correspond to the displacement fields enabling the calculation of effective parameters through spatial homogenization. The detailed procedure for characterizing Representative Volume Elements (RVEs) has been clarified in the *Methods* section of the main text, with reference to standard protocols [Okereke *et al.*].

Why use an orthotropic framework and C66 as the unique shear component?

We consider here structures involving symmetry at the supercell scale, which enables simplification of the elasticity tensors by canceling the coupling terms between axial deformations and shear ($C_{16} = C_{26} = 0$, and by symmetry $C_{61} = C_{62} = 0$). This simplification is only valid when the analysis is oriented along the principal axes of the inclusions in the supercells, otherwise, rotation tensors performing four-dimensional projections must be added. Considering the symmetry between the terms C_{12} and C_{21}, we thus have four degrees of freedom in this tensor, whose representation is simplified using the Mandel-Kelvin notation described in the article. To facilitate the physical interpretation of these quantities, we performed a diagonalization of the tensor to extract its principal behaviors, expressed again along its principal axes. This diagonalization has the effect of decomposing the cell's behavior into two axial effects along axes revealed by the diagonalization of the orthotropic tensor, as well as a shear effect.

The consideration of a simplification into orthotropic tensors finds numerous echoes in the scientific literature and proves effective even in potentially less favorable contexts where the composition of periodic cells evaluated during characterization corresponds to more complex geometries than our identically sized and oriented elliptical inclusions (see pixelated approach in Fig. 1b).

What are the database size and sampling strategy?

To complete Fig. 3 and better describe our procedure, we have added a specific section in the *Supplementary Materials* now constituted in the new version of our article.

Our generative model depends on input parameters. The parameters f and k determine the type of shape that emerges during growth and are kept constant. In connection with a previous comment and a detailed addition in the *Supplementary Materials*, the diffusion coefficients d_u

and d_v are also constant for all of this work in order to impose the maximum dimension of the elliptical inclusions as a function of the size of the growth domains. The control of emerging structures therefore depends on two parameters:

First, the anisotropy of the diffusion tensor, controlling the axial ratio of the ellipses emerging during pattern growth, is determined by the first eigenvalue λ of the diffusion tensor $\underline{\underline{\mathbf{D}}}$. To ensure mass conservation in this generative model, the trace of the tensor is normalized, ensuring that the first eigenvalue alone allows the value of the second to be deduced, defined as $1 - \lambda$.

Second, the binary segmentation threshold σ determines the porosity level of the structures by reducing the size of pores from the morphogenetic fields U and V, which are initially continuous.

The growth angle of the structures can also be controlled locally, but is kept constant and oriented along the horizontal axis. This simplification is permitted by considering that a rotation of the ellipses implies a simple change of reference frame that can ultimately be reflected by adding a rotation matrix to the results, and simultaneously allows canceling the coupling terms between normal and shear modes.

For Fig. 3e, the space of variable generative parameters σ and λ is therefore uniformly sampled, considering $\sigma \in [0, 1]$ including 11 samples and $\lambda \in [0.5, 0.8]$ including 11 samples.

For each simulation, a structure is generated and meshed on a torus to ensure spatial periodicity conditions (right side of Fig. 3e). For each structure, an elasticity tensor is determined by a series of three simulations, ultimately allowing, after diagonalization of the tensor, an sample to be obtained in the space of available solutions represented in Fig. 3e. Given the difficulty of interpreting these fourth-order tensors represented in two dimensions by Mandel-Kelvin notation, we finally opted for a representation along three axes.

The stiffness trace represents the sum of the eigenvalues of the tensor, i.e., the trace of each tensor $\underline{\underline{\mathbf{C}}}$. This metric reflects the overall stiffness of the structure.

Principal stiffness anisotropy corresponds to the ratio of the first two eigenvalues. This metric concretely represents the potentially different elastic behavior of the structures along their two principal axes.

Finally, the shear effect is represented by the component C_{66}, decoupled from the other components when the structure is analyzed along its principal axes.

To complete this analysis, a mapping of the components of the tensor $\underline{\underline{\mathbf{C}}}$ obtained as a function of the generative parameters is added in the *Supplementary Materials*.

Modifications made to the manuscript:

- **RVE characterization:** Clarified the procedure in the *Methods* section with relevant references (e.g., Okereke *et al.*).
- **Orthotropic assumption:** Added references justifying the orthotropic simplification and coupling term cancellation.

- **Equivalent model schematic:** Added references justifying the model and the link to the extensive database in the *Supplementary Materials*.
- **Parameter values:** Provided explicit values for f, k, d_u, and d_v parameters.
- **Tensor mapping:** Included a mapping of tensor $\underline{\underline{\mathbf{C}}}$ components as a function of generative parameters in the *Supplementary Materials*.

6. The authors should clarify the necessity of setting the parameter R2. Specifically, an explanation is needed regarding whether the mechanical steady state is achieved naturally by the model dynamics without explicitly prescribing R2.

To clarify, R_2 is not a parameter of the reaction-diffusion dynamics itself, but rather the outer radius defining the extent of the cloaking region (here $R_2 = 2R_1$, where R_1 is the hole radius). This choice follows conventions from the mechanical cloaking literature (references [24] and [25]) and defines the annular region over which the tensor transformation is applied.

The value of R_2 determines the size of the cloak and was simply chosen to correspond to the references indicated in the literature. Since this value is itself a fraction of the size of the growth domain, it does not really impose a constraint on the convergence of the reaction-diffusion process, but rather changes the values locally guiding the orientation and anisotropy of the self-duplicating and self-organizing patterns through the decentralized properties of our generative model. The reaction-diffusion patterns do achieve a steady state naturally through their intrinsic dynamics.

7. The data presented in Figures 5 and 6 show negative displacement in the tensile direction. This outcome is unconventional and appears erroneous. The calculation methodology for displacement must be clearly explained, as the current presentation suggests a departure from common practice.

A comment was already included to warn about the effect of such a choice but a more detailed description is now added in the *Supplementary Materials*. Surprisingly, the metrics obtained are more favorable when this symmetrization is not applied, but we preferred to propose an analysis carried out in a case more fairly comparable to other experiments in the literature. This choice corresponds only to a change of reference frame and therefore does not directly affect the data, but this comment indicates that it is important to provide the raw data from our experiments.

To address this concern, we have added the simulated raw displacement fields in the *Supplementary Materials*. Metrics are provided for both raw and symmetrized data to demonstrate the robustness of the conclusions.

Modifications made to the manuscript:

- **Symmetrization discussion:** Expanded explanation of the reference frame choice in the Main Text (Discussion section).
- **Raw data provision:** Addition of raw displacement fields in the *Supplementary Materials* (Section "Symmetrization of Displacement Fields").

8. Since the authors are solving a design and optimization problem, the mathematical definition of the problem (i.e., the objective function, design variables, and constraints) must be explicitly stated.

While our approach involves design objectives, it differs fundamentally from conventional topology optimization formulations. Our method represents a generative approach where the design emerges from morphogenetic principles rather than through iterative gradient-based optimization. Nevertheless, we recognize the need to formalize the problem statement mathematically to clarify how our approach achieves its objectives. This question addresses three aspects: the formulation of design objectives, the identification of design variables, and the specification of constraints.

How is the design objective formulated?

Our objective is to synthesize spatial distributions of local stiffness tensors $\underline{\underline{\mathbf{C}}}(\mathbf{x})$ that match target tensors $\underline{\underline{\mathbf{C}}}'(\mathbf{x})$ obtained from the transformation-based cloak design. Unlike classical topology optimization, we do not define an explicit objective function to be iteratively minimized. Instead, we construct a pre-computed database mapping morphogenetic parameters to homogenized elastic tensors, and select parameters pointwise based on proximity to the target in the space of tensor invariants (trace, anisotropy, orientation). The "optimization" is thus reduced to a single database lookup operation per spatial location, without iterative feedback.

What are the design variables?

The design variables in our framework are the local morphogenetic parameters that control the reaction-diffusion growth: the diffusion anisotropy $\lambda(\mathbf{x})$, the binary segmentation threshold $\sigma(\mathbf{x})$, and the orientation angle $\theta(\mathbf{x})$. These parameters are spatially varying fields that guide the self-organization of elliptical patterns. Once assigned based on the target tensor field, these parameters are fed to the reaction-diffusion engine, which generates the final microstructure through purely local interactions without requiring global equilibrium solves or sensitivity analysis.

What are the constraints?

The constraints in our approach are implicit and embedded in the database construction. The database itself encodes physical realizability: each entry corresponds to a microstructure that has been numerically homogenized and verified. The restricted parameter ranges (e.g., $\lambda \in [0.5, 0.85]$ to avoid pore merging, $\sigma \in [0, 1]$ for porosity control) represent manufacturability constraints. Spatial smoothing of the parameter fields ensures continuity of the microstructure and compatibility between neighboring regions. Unlike gradient-based methods that enforce constraints through Lagrange multipliers or penalty functions, our constraints are naturally satisfied by construction through the emergence of self-organized pores.

Modifications made to the manuscript:

- **Generative paradigm:** Added clarification in *Methods* emphasizing the non-iterative, generative nature of the approach.
- **Feedback decentralization:** Emphasized the absence of centralized iterative feedback guiding structural evolution.
- **Biological analogy:** Highlighted the analogy with morphogenesis in living systems (bottom-up emergence vs. top-down calculation).

9. The absence of the finite element mesh makes it difficult to ascertain the model's accuracy. Since the model is inherently 3D despite the results being presented in 2D, a visualization and description of the overall mesh resolution are crucial for validating the computational results.

We thank the reviewer for insightful comment, which helped us enhancing the metrics presented in the article. We performed a rigorous mesh convergence study using 3DEXPERIENCE with quadratic tetrahedral elements (C3D10). We refined the mesh density to capture local stress gradients around the holes and fillets, which slightly improved the agreement between simulation and experiment. Specifically, the relative bias β on the improvement factor dropped from 13% to **6.2%**. These new results are now detailed in the *Supplementary Materials* (Section "Meshing and Numerical Accuracy").

Modifications made to the manuscript:

- Added the convergence study and mesh details to *Supplementary Materials*.
- Updated the relevant metrics in the text (relative bias β = 6.2%).

10. The meaning and methodology for evaluating the homogenized elastic constants from corner-node reactions and displacements must be clearly defined and explained, as this is an unconventional approach for calculating effective material properties.

Our approach follows standard periodic homogenization theory but may not have been presented with sufficient methodological detail. This question addresses two aspects: the theoretical framework of periodic homogenization that justifies our approach, and the practical implementation through corner-node reactions and displacements.

What is the theoretical framework for periodic homogenization?

The homogenization procedure is based on the concept of a Representative Volume Element (RVE), which assumes that a sufficiently large periodic cell can capture the effective mechanical behavior of the heterogeneous microstructure. Under periodic boundary conditions, opposite faces of the RVE undergo identical deformations but with opposite forces, ensuring compatibility and equilibrium at the macroscopic scale. This framework is well established in the literature for extracting homogenized properties from periodic microstructures. By applying prescribed displacement-controlled loading along different directions (uniaxial and shear), we can systematically extract all independent components of the effective elasticity tensor. The procedure is detailed in the *Methods* section, citing standard works such as [Okereke *et al.*] on RVE characterization:

Okereke, M. I., & Akpoyomare, A. I. (2013). A virtual framework for prediction of full-field elastic response of unidirectional composites. Computational materials science, 70, 82-99.

How is the corner-node method implemented?

In practice, we implement periodic boundary conditions through multi-point constraints that tie opposite faces of the RVE. The corner nodes play a special role: they serve as reference points where we apply controlled displacements to impose the desired macroscopic strain state. The reaction forces at these corner nodes, combined with the imposed displacements, directly yields the homogenized stress-strain relationship. Specifically, for each load case (horizontal tension, vertical tension, shear), we compute the effective stiffness coefficients from the ratio of averaged stress (computed from corner-node reactions) to applied strain (imposed through corner-node displacements). This approach is computationally efficient and ensures that the extracted properties satisfy reciprocity and symmetry conditions inherent to elastic behavior. We take this opportunity to reiterate that our entire characterization pipeline is freely available to readers interested in a more in-depth analysis of our methodology. We hope that this contribution will facilitate the reproduction and wider dissemination of this work.

Modifications made to the manuscript:

- **Corner-node method:** Included a brief mention and description of the corner-node implementation in the Methods section.
- **Characterization pipeline:** Created a dedicated section in the *Supplementary Materials* describing the generation, meshing, and simulation procedure for extracting elasticity parameters.

11. The periodic unit cell microstructure employed contains a notably large number of holes. The authors should justify why this high density is necessary; it is generally sufficient to use a minimal number of representative holes within the unit cell to adequately capture the effective material behavior.

Regarding the representative volume element (RVE) size and the number of inclusions needed for proper homogenization, since generation is performed without uniformity constraints, the extraction of local parameters is calculated using the principle of supercells.

Following a series of self-duplications and progressive self-organization of the elliptical elements, they systematically converge toward an arrangement with uniform spacing. To ensure periodicity conditions in two dimensions, this growth is performed on a torus. When the size of the growth domain is small relative to the dimensions of the patterns, they may experience greater pressure from their neighbors due to the self-organization effect inherent to our generative model. This pressure can translate into a slight variation in the distance between pores once segmentation is performed, slightly altering the expression of the obtained parameters. We therefore propose to perform these characterizations on domains containing several pores per side of the supercell, attenuating the pressure of cells on their neighbors and allowing spacing much closer to that obtained during large-scale growth.

To improve the construction of our databases, we also employ two additional mechanisms to limit the impact of the growth domain on the expression of effective parameters.

First, the first eigenvalue of the diffusion tensor varies symmetrically around the isotropic case $\lambda = 0.5$ where circular patterns are generated. This symmetry in the dataset allows us to average results and improve statistical representativeness.

Second, the data are averaged over multiple random initializations of each generation, further reducing sensitivity to initial conditions and improving the robustness of the extracted homogenized properties.

We have also clarified that RVE characterizations are performed on supercells containing 5 patterns per side to mitigate boundary effects. Additionally, we specify in the *Supplementary Materials* that database entries are averaged over symmetrical variations of the anisotropy parameter and multiple random seeds to ensure statistical robustness.

Modifications made to the manuscript:

- **Homogenization references:** Added references for the supercell principle in homogenization (*Methods*).
- **Mesh/RVE details:** Clarified RVE characterization on supercells (*Methods*) and detailed the statistical averaging of database entries (*Supplementary Materials*).

12. The authors state the use of 3D EXPERIENCE for the finite element analysis. It should be explicitly confirmed whether the underlying solver used is ABAQUS Standard and the specific version number must be included for reproducibility.

We have updated the manuscript to clarify the distinction between the tools used. The 2D material database was generated using ABAQUS Standard under plane stress conditions to determine the effective properties of the supercells. The 3D full-cloak simulations were performed using the 3DEXPERIENCE platform (SIMULIA), allowing for a high-fidelity 3D model that includes rigid steel bars to mount the POM and clamping effects, reproducing the experimental boundary conditions with greater accuracy.

Modifications made to the manuscript:

- **Solver identification:** Added explicit mention of ABAQUS Standard as the primary solver in the *Methods* section.
- **Reproducibility:** Specified solver settings, versions, and convergence criteria used for the numerical simulations.

We hope that these detailed responses have addressed the specific concerns you raised. We would like to conclude by emphasizing the fundamental paradigm shift that our method represents compared to conventional optimization approaches.

Our technique is a self-organized, fully decentralized method that breaks with conventional optimization methods based on incremental improvement at large scale. Traditional methods involve centralized feedback, evaluation of distance to a cost function that is iteratively minimized, requiring significant computational resources and limiting the scalability of the obtained structures. Here, structuring is achieved through local rules, without requiring new large-scale simulations to converge toward the desired characteristics. Moreover, the self-duplication and self-organization properties guaranteed by this generative model ensure significant robustness to initial conditions and manufacturing defects, while offering the flexibility of a topology that progressively adapts to the available space and local constraints.

We thank you again for your thorough and constructive review of our work. We hope that the clarifications and additions provided have convinced you of the relevance of our approach and have provided all the necessary elements for a proper evaluation of our contribution.

2 Reviewer #2

This paper presents a morphogenesis-inspired optimization approach for designing a mechanical cloak. The authors present their simulation results along with experimental validation. They also compare their results with previously published approaches. The work is interesting and ties together optimization, simulations, and experiments. However, there are points for improvement, particularly to address the broad readership of Nature Communications.

We appreciate the constructive suggestions to improve accessibility for the broad readership of Nature Communications. We have carefully addressed each point raised, focusing on clarifying key concepts, improving figure presentation, reorganizing the validation section, and correcting formatting issues. The modifications made are detailed below in our point-by-point responses.

1. The authors should consider updating the introduction to address the broad readership of Nature Communications. In particular, please provide clear definitions for the terms mechanical cloak and morphogenesis.

We acknowledge that clear definitions of these central concepts are essential for a broad readership. *Introduction* to provide accessible definitions of both mechanical cloaking and morphogenesis early in the text.

Modifications made to the manuscript:

- **Definitions:** We added explicit definitions of ”mechanical cloak” and ”morphogenesis” in the *Introduction*.

2. On a similar note, Figure 1 could be improved to be more illustrative of the high level concept of the paper.

We appreciate this suggestion. In retrospect, the organization initially proposed, blending the fundamental concepts of our approach with cloaking, was likely not optimal. To improve clarity, we have consolidated all elements related to our generative model into Figure 2 and updated the associated captions accordingly.

Modifications made to the manuscript:

- **Figure 1 and 2 redesign:** We have restructured the figures to separate the high-level concept from the technical implementation. Figure 1 now focuses exclusively on the conceptual framework, while the specific details regarding the generative model have been moved to Figure 2. Both captions have been revised to reflect this reorganization.

2.1 Much of Figure 1 is described in the Introduction, but the figure is not referenced in the text until Results.

Indeed, the figure appeared disconnected from the early text. In the revised manuscript, we now explicitly reference Figure 1a and 1b in the Introduction when discussing existing approaches, and Figure 1c-e when introducing our morphogenesis-inspired concept. This ensures that the figure supports the narrative from the very beginning.

Modifications made to the manuscript:

- **Early referencing:** We now reference Figure 1a-b (existing approaches) and Figure 1c-e (our concept) directly in the Introduction to guide the reader.

2.2 How was the image in Figure 1c generated?

This figure (now 2a) was generated using Blender, a 3D computer graphics software. It represents a particle model corresponding to a reaction-diffusion system, two species interacting and achieving a random walk through space. This lagrangian description is substituted by an eulerian approach using discretized space with concentration of particles, implementing our model with finite differences.

3. The organization of the Validation section could be improved. For example, the values for Δ_{hole} and Δ_{cloak} from the simulations are not mentioned until the very end of the discussion comparing the experimental and simulation results. Please rework this section to make the comparison clearer.

We have restructured the Validation section to present the numerical performance metrics (Δ_{hole} and Δ_{cloak}) immediately alongside the simulation results. We then present the experimental metrics in the following subsection, allowing for a more logical flow. A specific discussion paragraph now bundles the comparison, highlighting the consistency between numerical predictions and experimental findings.

Modifications made to the manuscript:

- **Restructuring:** We reorganized the Validation section to present experimental and simulation metrics (Δ) immediately after their respective results.
- **Comparative summary:** We grouped the discussion of improvement factors in a dedicated subsection ”Consistency between simulation and experiment”.

3.1 It would be interesting to see the experimental and simulation results for the 3 samples compared side by side in a figure (i.e. combining Figures 5 and 6). The authors might consider adding this to either the main text or supplementary material.

A side-by-side comparison significantly aids in visual verification, as suggested. We have modified the Main Text to include side-by-side comparisons of the experimental and simulation results in Fig. 5 and Fig. 6. This direct visual comparison reinforces the quantitative agreement reported in the text.

Modifications made to the manuscript:

- **Side-by-side comparison:** We updated Fig. 5 (u_1) and Fig. 6 (u_2) in the Main Text to present the experimental and simulation results side-by-side for the Reference, Hole, and Cloak cases, enabling direct visual verification of the cloaking performance.

4. Regarding the comparison presented in Table 1, could the authors comment on how different loading types and boundary conditions might change the calculated effectiveness of a mechanical cloak, as well as if these would affect the agreement between simulations and experiments?

We agree that quantitative metrics are sensitive to boundary conditions, but we believe the best way to address this concern is to demonstrate that the *intrinsic* cloaking capability of our generated structures remains robust across completely different loading scenarios. To this end, we have significantly expanded our validation beyond the initial tensile test.

1. Generalization to six distinct loading scenarios:
We have subjected the *single exact same structure* (originally generated for the tensile case) to five additional and disparate boundary conditions:

- Uniaxial Compression
- Confined Compression
- Simple Shear
- Equibiaxial Tension
- Standard Uniaxial Tension

As detailed in the new ”Analysis of six loading cases” section of the *Supplementary Materials*, the result is striking: the generated metamaterial systematically reduces the displacement error compared to the hole, regardless of the loading mode. This confirms that the morphogenetic process successfully synthesizes a material distribution that mimics the background medium's constitutive behavior properly, rather than fitting a specific boundary value problem.

2. Robustness to generation conditions (Resolution & Stochasticity):
In addition to loading types, we also investigated the sensitivity to the generation process itself. We performed a large-scale statistical study involving:

- 10 random seeds per loading case: verifying that performance is deterministic despite the stochastic local pore distribution.
- 3 distinct resolutions (603^2, 1005^2, 1407^2 pixels): verifying that the method is scalable and that performance actually improves with finer microstructures.

These results, summarized in Fig. C1 of this letter and detailed in the *Supplementary Materials*, provide strong evidence that the agreement between simulation and experiment is not an artifact of a specific setup, but a robust feature of the proposed method.

Modifications made to the manuscript:

- **Extensive Validation:** Added a comprehensive section in the *Supplementary Materials* ("Analysis of six loading cases with the mechanical cloak") presenting statistical results (mean & std. dev) for the 6 loading scenarios and 3 resolutions.
- **Database Equivalence:** Added a verification section ("Equivalence of Tension and Compression Databases") demonstrating that the stiffness databases are valid for both tension and compression, justifying the single-structure approach.
- **Discussion:** Expanded the main text discussion to highlight this multi-scenario robustness as a key differentiator from standard topology optimization which is often load-case specific.

4.1 The authors should consider adding an example using their system for a mechanical cloak under compression, for a more direct comparison with Ref 24.

Following this recommendation, we have now added now compressive loading results to the manuscript and the *Supplementary Materials*. They demonstrate that the morphogenetic cloaking principle remains effective in compression, yielding performance metrics comparable to the tensile case and allowing for a fair comparison with the literature benchmarks.

Modifications made to the manuscript:

- **Compression validation:** Detailed in the *Supplementary Materials* ("Generalization" section), we constructed a compression-equivalency database and simulated the cloak under compressive loading, demonstrating robustness.

5. Please comment further on potential applications of this work.

We have expanded the Discussion section to articulate three key axes of application: (1) **Scalability**: the ability to generate massive, continuous metamaterials for large-scale architectural or aerospace components without mesh-dependency issues; (2) **Versatility**: the extension to stress field guiding (as demonstrated with the bridge and cantilever examples) for structural optimization; and (3) **Robustness**: the potential for defect-tolerant designs in additive manufacturing, leveraging the self-organization properties to heal or adapt to local irregularities.

Modifications made to the manuscript:

- **Applications outlook:** We expanded the Discussion to include three key pillars: Scalability (large domains), Versatility (stress guiding, compression), and Robustness (defect tolerance).
- **Future directions:** We briefly outlined potential extensions to 3D and wave control applications.

6. Formatting/grammar points to be addressed:

6.1 There are several typos scattered throughout the text.

We have conducted a thorough proofreading pass and corrected all identified typographical errors throughout the manuscript. We have also used automated spelling and grammar checking tools to ensure consistency.

Modifications made to the manuscript:

- **Proofreading:** We conducted a global spell-check and grammar review of the document.

6.2 Additionally, there is inconsistent capitalization and formatting of journal titles in the references.

We have reviewed all references and standardized the formatting according to Nature Communications style guidelines. All journal titles now follow consistent capitalization (title case for major words), italicization, and abbreviation conventions.

Modifications made to the manuscript:

- **Bibliography normalization:** We standardized all references to comply with Nature Communications format (journal abbreviations, italics, capitalization).

6.3 There are a few places in the Introduction/Results sections where there are minor repeated phrases.

We have carefully reviewed the Introduction and Results sections and removed all repeated phrases. These repetitions likely arose during iterative editing and revision. The text now flows more smoothly without these unnecessary redundancies.

Modifications made to the manuscript:

- **Text cleaning:** We removed redundant phrases in the Introduction and Results sections to improve flow.

6.4 Equations would be better presented in the text as opposed to in figures (Figure 3d).

Considering your recommandation, we have extracted the equations from Figure 3d and incorporated them into the main text as properly numbered equations in the *Methods* section. Figure 3d now serves as a schematic illustration of the database construction concept, with the mathematical formulation presented separately in the text where it can be properly referenced and discussed. This change improves both readability and the professional presentation of the mathematical content.

Modifications made to the manuscript:

- **Equation formatting:** We extracted the database generation equations from Figure 3d and integrated them into the *Methods* section text for better readability and referencing.

We thank Reviewer #2 again for these constructive and detailed suggestions. The modifications addressing these points have significantly improved the accessibility and presentation quality of our manuscript for the broad readership of Nature Communications.

3 Reviewer #3

The manuscript proposes a decentralized, morphogenesis-inspired generator for mechanical metamaterials whose local effective elasticity is steered by anisotropic reaction–diffusion. A precomputed database links generative parameters to homogenized stiffness matrices. An orthotropy-preserving tensor transformation maps a cloak design into target local tensors. The nearest database entries are assigned pointwise, smoothed, snapped to realizable values and then the microstructure "self-organizes". The approach is validated by a mechanical cloaking experiment.

The conceptual contribution is valid and results in fabricable designs, however there lacks sufficient numerical or experimental evidence that the method is robust. I suggest the following:

We appreciate the recognition of the validity of our conceptual contribution and the questions regarding numerical robustness. We address each point systematically below, providing additional numerical evidence and clarifications that strengthen the validation of our approach. These additions are presented in expanded *Supplementary Materials* sections.

1. How closely do realized tensors match the targets? Can you propose an error metric (trace, anisotropy, shear and principal-direction misalignment)

To quantify the accuracy of our tensor matching procedure, we now provide comprehensive error profiles for all tensor components in the *Supplementary Materials* and present two new complementary analyses.

What does the convergence analysis from database lookup show?

We first analyze the convergence of our approach as presented in response to Reviewer #1, Question 1, which is detailed in the *Supplementary Materials*. This analysis demonstrates that the database lookup and smoothing procedures systematically converge toward realizable tensor distributions that closely approximate the transformation-based targets.

What are the spatial error metrics for tensor components?

We have computed radial error profiles throughout the cloaking domain for the following quantities:

- *Trace error:* $\epsilon_{\text{tr}}(\mathbf{x}) = |\text{tr}(\underline{\underline{\mathbf{C}}}(\mathbf{x})) - \text{tr}(\underline{\underline{\mathbf{C}}}'(\mathbf{x}))|/\text{tr}(\underline{\underline{\mathbf{C}}}'(\mathbf{x}))$
- *Anisotropy error:* $\epsilon_{\text{anis}}(\mathbf{x}) = |\eta(\mathbf{x}) - \eta'(\mathbf{x})|$ where $\eta = \lambda_1/\lambda_2$ is the eigenvalue ratio
- *Shear error:* $\epsilon_{\text{shear}}(\mathbf{x}) = |C_{66}(\mathbf{x}) - C'_{66}(\mathbf{x})|/C'_{66}(\mathbf{x})$

- *Principal direction misalignment:* $\epsilon_\theta(\mathbf{x}) = \arccos(|\mathbf{v}_1 \cdot \mathbf{v}_1'|)$ where $\mathbf{v}_1$ and $\mathbf{v}_1'$ are first eigenvectors

For each metric, we provide a companion figure in the *Supplementary Materials* showing the radial distribution of the target vs. realized properties. These visualizations reveal that trace, anisotropy, and principal direction matching are excellent throughout the domain. Shear matching is less accurate, particularly approaching the hole center, despite our use of techniques avoiding singularities and divergence in the transformation method. This anticipated limitation is discussed further in response to Question 2.

What is the important caveat regarding periodic boundary condition effects?

It is important to note that these tensor parameters are deduced from structures characterized under periodic boundary conditions in the database construction phase. Additional distortions likely occur when generating the full cloak, where neighboring cells are not identical to the local cell. We do not currently have a direct method to extract these local elasticity coefficients from the complete non-periodic structure without performing prohibitively expensive local RVE extractions throughout the domain. The presented metrics therefore represent an upper bound on matching accuracy based on the database entries selected.

Modifications made to the manuscript:

- We added a new section in *Supplementary Materials* providing radial error profiles for Trace, Anisotropy, and Orientation.

2. The matching is only done using the trace and principal direction, and anisotropy and shear "follows implicitly". How would you then independently control the latter two as you state in the paper? Can you justify why this is chosen as the method.

To clarify our matching strategy: we actually control trace, principal direction, *and* anisotropy. Shear is indeed the component that "follows implicitly" rather than being independently controlled, and this choice merits detailed justification.

Our database lookup matches three quantities: the stiffness trace (controlling overall rigidity), the anisotropy ratio $\eta = \lambda_1/\lambda_2$ (corresponding to the eigenvalue ratio of the Jacobian operator, ultimately translated into the eigenvalue ratio of the diffusion tensor guiding generation), and the principal direction alignment θ. These three parameters directly map to the generative parameters σ (porosity via binary segmentation threshold), λ (diffusion anisotropy), and θ (local growth orientation).

Why is shear not independently controlled: fundamental limitations of transformation elasticity?

The limitation regarding independent shear control stems from the fundamental nature of mechanical governing equations. Transformation-based methods were originally developed in electromagnetics, where the governing equations exhibit form-invariance under coordinate transformations and where the constitutive tensors are generally of lower order. In elasticity, the situation is fundamentally more complex: the constitutive relation links a fourth-order tensor to second-order strain and stress tensors, and the equations are not form-invariant under arbitrary transformations.

We address this challenge through two relaxation strategies:

First, we work in the principal reference frame of orthotropic structures, simplifying tensor representation using Mandel-Kelvin notation and minimizing coupling between bulk and shear modes (the off-diagonal terms C_{16}, C_{26} vanish by symmetry).

Second, we restrict ourselves to *diagonal* Jacobian transformations, meaning we only locally modify global stiffness and anisotropy without rotating the principal stress and strain field directions. This constraint significantly simplifies the transformation problem.

Under these conditions and with weak coupling to shear parameters, we have demonstrated that effective cloaking can be achieved by controlling only the bulk parameters (trace, anisotropy, orientation). Independent control of shear parameters would require either special geometries ensuring complete decoupling (such as pentamode materials) or layered combinations of orthotropic structures, which would add significant complexity to this proof-of-concept demonstration.

What is the validation strategy and future work?

For simplification and to provide an effective validation, we identified the degrees of freedom most significant for this experiment. Future work will generalize these mathematical transformations and explore generation of more complex forms enabling fuller tensor control. As additional supporting evidence requested by Reviewers #1 and #2, we provide complementary application contexts: numerical cloaking under compression and numerical stress field guidance experiments, both demonstrating robustness of the bulk-parameter-focused approach.

Modifications made to the manuscript:

- **Clarification:** We revised the *Methods* section to explicitly state that we control Trace, Anisotropy, and Orientation, while Shear is implicitly determined by the orthotropic symmetry.
- **Discussion:** We added a paragraph discussing the fundamental limitations of transformation elasticity compared to electromagnetics regarding shear decoupling.

3. Can you quantify the coverage in terms of elasticity tensor that is realizable with the method? Both in terms of how finely controllable the resulting elasticity is, and how wide the coverage is.

We now provide a more comprehensive characterization of both the controllability resolution and the coverage extent. We have presented a synthetic representation of the parameter space achievable with our approach for a base material with Young's modulus $E = 3$ GPa and Poisson's ratio $\nu = 0.35$ (POM). We now provide in the *Supplementary Materials* a clearer representation of the generation parameter space employed for this demonstration, as well as its relationship to the space of attainable mechanical parameters, within the limits of the numerical conditions explored in this context.

What is the coverage extent (range of accessible properties)?

The database samples the generative parameter space with $\sigma \in [0, 1]$ (11 samples) and $\lambda \in [0.5, 0.8]$ (11 samples). The compression and tension databases are now provided in the *Supplementary Materials*.

What is the controllability fineness (resolution)?

The discrete sampling with $11 \times 11 \times$, combined with the smoothing and interpolation steps, provides effective continuous control. The smoothness of the mapping between generative and mechanical parameters (discussed in Question 4) ensures that intermediate property values can be reliably targeted.

What about extensibility and future work?

The demonstrated bounds can be readily extended in future work. Broader coverage would require advancing the generative models to produce more complex forms (e.g., non-elliptical pores, hierarchical structures) while maintaining the self-duplication and self-organization properties exploited here. Finer controllability can be achieved simply by denser sampling of the (σ, λ) space, though the current resolution already proves sufficient for the cloaking application.

Modifications made to the manuscript:

- **Parameter space visualization:** We added 3D scatter plots in the Main Text and detailed 2D maps in the *Supplementary Materials* illustrating the accessible domain in the (Trace, Anisotropy, Shear) space covered by our database.

4. Can you discuss the possibility of multiple distinct geometries all exhibiting similar tensorial quantities? Second, will a small perturbation in lambda, sigma or theta change the geometry greatly?

This question addresses two critical concerns: the uniqueness of the generative-to-mechanical mapping (the notorious many-to-one problem in inverse design) and the sensitivity of the approach to parameter perturbations.

Is there uniqueness within the explored parameter space?

Within the conditions specified and the domain explored (as detailed in the *Supplementary Materials*), we do not observe multiple candidate geometries with different generative parameters leading to identical mechanical parameters. The converse is also true, implying a bijection of the operator relating generative and mechanical parameters within these restricted spaces.

The mapping is therefore direct, and the operator exhibits favorable properties for our application: the spaces are smooth, exhibit no discontinuities, and display monotonic behavior (i.e., increasing σ monotonically decreases porosity and increases stiffness, increasing λ monotonically increases anisotropy).

Are there alternative parameterizations and extended degeneracy?

However, it is possible to propose alternative parametric variations that produce different structures with substantially equivalent properties. For example, changing the diffusion coefficients d_u and d_v impacts the periodicity of generated patterns (see new mathematical development in *Supplementary Materials* for proof). Under these conditions, a pair of values (diffusion coefficient d_u, segmentation threshold σ) can lead to characteristics substantially close to those from another parameter pair, imposing a new geometry. We provide a practical example of this degeneracy in the *Supplementary Materials*.

What is the sensitivity to small perturbations?

Regarding small perturbations, the operators being smooth (technically: the mapping $(\sigma, \lambda) \mapsto (\text{trace}, \eta, C_{66})$ is continuously differentiable), the relationships are locally linear. Small perturbations in generative parameters therefore induce small perturbations in the associated mechanical parameters.

It is important to note, however, that fairly different geometries can be obtained in the absence of uniformity constraints on our generations. A macroscopic analysis will nevertheless systematically reveal that the dimensions, axial ratios, and orientations of the generated ellipses follow the locally imposed constraints. The morphogenetic process introduces stochastic microstructural variations (pore positions, exact shapes) that do not significantly affect the homogenized mechanical properties, demonstrating robustness.

Modifications made to the manuscript:

- **Mathematical proof:** We added a derivation in the *Supplementary Materials* linking diffusion coefficients to pattern periodicity, demonstrating the origin of geometric variations.
- **Robustness discussion:** We expanded the *Discussion* to clarify that stochastic variations in microstructure do not significantly degrade homogenized properties, as evidenced by our 10-seed study.

5. The cloak example is only valid under uniaxial tension for one hold radius. Can you show (at least numerically) more examples, such as shear loading, biaxial tension, or non-circular cavity?

We thank the reviewer for this crucial suggestion. Indeed, demonstrating robustness beyond the single configuration originally presented is essential to validate the approach. We have therefore significantly expanded our validation scope in two key directions:

1. Robustness of the Cloaking Performance (6 new test cases):
We have extended the numerical analysis of the exact same cloak design (optimized for uniaxial tension) to six additional mechanical loading scenarios, including confined compression (sliding and symmetric), simple shear, equibiaxial tension (dilating mode), and tension without lateral contraction. These results are detailed in the new section *"Analysis of six loading cases with the mechanical cloak"* of the *Supplementary Materials*. The cloaking performance is maintained across these disparate conditions without requiring any re-optimization. This confirms that the synthesized heterogeneity effectively mimics the background material response even under loadings different from the design case.

2. Generalization to Stress-Guided Optimization:
To demonstrate the versatility of the method beyond pre-calculated cloaks and circular cavities, we applied our "stress-guided growth" strategy to two classic structural optimization problems: a *Cantilever Beam* and a *Distributed Bridge*. As detailed in the *Supplementary Materials* ("Analysis of Stress-Field Guided Growth") and illustrated in the Main Paper (Fig. 12), the method spontaneously generates optimized truss-like structures aligned with principal stress trajectories. A key advantage is that these complex architectures are grown in a "one-shot" process requiring only a few seconds of computation, offering a scalable alternative to iterative topology optimization.

Modifications made to the manuscript:

- **Expanded Cloaking Validation:** We added a comprehensive section in the *Supplementary Materials* ("Analysis of Mechanical Cloaking Performance") presenting numerical results for 6 additional loading cases (compression, shear, biaxial tension) to demonstrate the robustness of the reference cloak.

- **Stress-Guided Optimization:** We introduced two new application cases (Bridge and Cantilever) in the *Supplementary Materials* to demonstrate the method's extensibility to general structural optimization problems.
- **Main Text Update:** We added a description of these new results in the Results section and included a representative figure (Fig. 12) illustrating the stress-guided growth.

6. Can you provide a more balanced comparison between results generated from a topology optimization type algorithm (Table 1)?

The comparison with topology optimization in Table 1 was intended to benchmark the reliability of the numerical predictions (agreement factor β) rather than the absolute performance metrics (Δ), given the vastly different boundary conditions. The topology-optimized structures in Ref. [24] benefit from idealized boundary conditions (sliding rollers) that are difficult to realize experimentally, yielding lower theoretical errors. Our setup, using clamped boundaries, inherently induces larger reference displacements. To provide a more balanced perspective, we have revised the text to explicitly state that our method targets *scalability* and *manufacturability* (via "one-shot" generation) rather than the absolute optimality achievable by iterative topology optimization. We also highlight that our refined simulations (Table 2) now show a high Sim/Exp agreement with only 6.2% relative bias β on the improvement factor.

Modifications made to the manuscript:

- **Table 1 Clarification:** We revised the caption of Table 1 to explicitly state that it compares the *experimental validation agreement* (β factor) rather than absolute cloaking performance, due to the disparate boundary conditions across studies.
- **Text revision:** We clarified in the text why direct performance comparison with topology optimization is methodologically constrained by the differing boundary conditions (lateral pressure vs free edge).

7. The 3D claim is a bit speculative, I can forsee some fundamental difficulties in extending this. Can you discuss this a bit more?

Surprisingly, the transition of these works seems rather direct in 3D, both for the generative model and for the effective synthesis of orthotropic mechanical tensors. The reaction-diffusion as a generative model seems indeed agnostic of the type and dimensions of meshes considered for our finite difference models. The main challenge for the generative part consists in formulating an anisotropic diffusion operator in 3D, capable of imposing preferred directions for chemical component migration and guaranteeing mass conservation. We have not yet found a source in the literature that mentions clearly such an operator, but our successfull implementation confirmed that the transition to anisotropic generation in 3D is indeed possible (Fig. C3). Concerning the mechanical part, it seems then possible to transpose our previous efforts to fourth-order tensors containing more coefficients, maintaining orthotropic characteristics limiting couplings between axial and shear modes by imposing common orientations and anisotropies at the scale of our supercells.

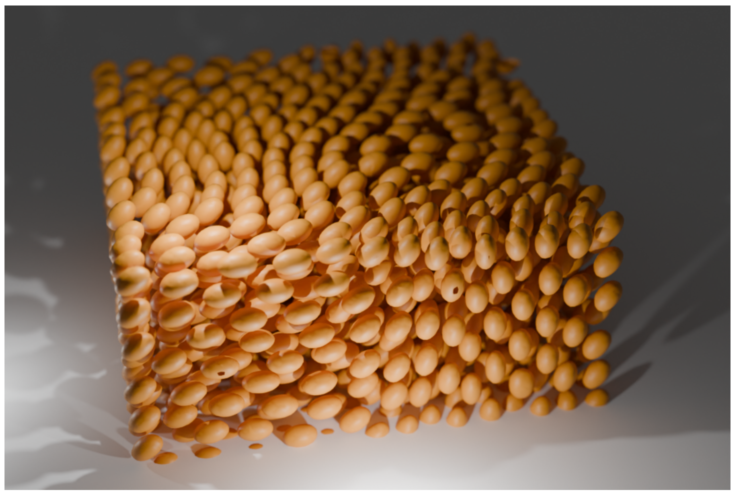

Figure C3: Proof-of-concept: 3D anisotropic morphogenetic structure generated using the proposed reaction-diffusion framework, demonstrating direct extensibility to volumetric domains.

We thank Reviewer #3 for their valuable feedback, particularly regarding the need for quantitative error analysis and the clarification of the 3D extensibility. Identifying these shortcomings has allowed us to significantly strengthen the validation of our approach and better articulate its generalization potential. We hope that the additional data and discussions provided in the revised manuscript satisfactorily address these concerns.

Sincerely,
Thomas Fromentèze, on the behalf of all authors

Morphogenetic mechanical metamaterials

Emerging tensor properties from self-organized structures

Correspondence with the anonymous reviewers

Thomas Fromentèze,[1,2,*] **Philippe Michaud,**[3]
Ali Hassny,[4] **and Vincent Pateloup**[3]

[1] University of Limoges, CNRS, XLIM, UMR 7252, F-87000 Limoges, France

[2] Institut Universitaire de France (IUF)

[3] University of Limoges, CNRS, IRCER, UMR 7315 , F-87000 Limoges, France

[4] University of Limoges, IUT du Limousin, F-87000 Limoges, France

[*] Corresponding author: thomas.fromenteze@unilim.fr

We thank the Editor and the Reviewers for their continued evaluation of our manuscript. We appreciate the constructive feedback provided in this subsequent review phase, which has allowed us to further improve the presentation of our work and clarify the remaining methodological points.

In response to the reviewers' recommendations, we have focused our efforts on enhancing the accessibility of our manuscript for the broad readership of Nature Communications. We have also refined our visual representations according to best practices, and provided further clarifications regarding our mechanical analysis framework, notably concerning tensor invariance and related metrics.

We hope that these adjustments address the remaining interrogations and strengthen the impact of our contribution. Below, we provide a point-by-point response detailing the specific clarifications and the corresponding modifications made to the manuscript, which are highlighted in blue in the revised document.

1 Reviewer #1

The authors have revised the manuscript in accordance with the reviewers' comments. While certain sections require further clarification, the majority of the requested revisions have been addressed, resulting in a notable improvement in the quality of the work. However, the following three points remain insufficient, and the reviewer requests that the authors address these concerns in a subsequent revision.

Specific Comments for Improvement:

5. Figure 3 Analysis: First, panels (a), (b), and (c) present deformation and distribution diagrams derived from finite element analysis; however, a legend for the distribution is missing.

We thank the reviewer for this constructive observation. It gives us the opportunity to clarify the theoretical foundations of the metrics used in our parametric space. We share the reviewer's concern regarding the necessity of using coordinate-independent quantities to characterize anisotropic materials, as orientation-dependent metrics would undermine the general applicability of the results. This comment raises three points that we address separately: the nature of the distributions in panels (a)-(c), the invariance of the metrics and the choice of anisotropy ratio, and the quantification of the shear stiffness range.

Quantities and scales represented in the distribution diagrams (a)-(c)

As requested, we acknowledge the missing legends in panels (a), (b), and (c). Colorbars specifying the magnitudes involved have now been added to the revised manuscript. We specify that we chose to normalize these displacement fields because the absolute displacement values depend heavily on the arbitrary size of the modeled supercell and have no direct physical significance for the subsequent extraction of the elasticity tensor components.

Are the characterized metrics rigorously invariant under coordinate transformation?

To address this requirement, we emphasize that the metrics presented in Figure 3e are not coordinate-dependent matrix components, such as C_{11}, C_{12} or C_{66} in Voigt notation, but are constructed exclusively from the invariant eigenvalues of the 4^{th}-order elasticity tensor.

The rigorous invariance of these quantities is guaranteed by the combination of two defining features of our methodology:

1. **Evaluation in the principal orthotropic axes**: All the generated supercells are systematically characterized in their unrotated configuration, where the elliptical inclusions are perfectly aligned with the global X-Y axes. In this principal frame, the homogenized orthotropic elasticity tensor presents no normal-shear coupling ($C_{16} = 0$ and $C_{26} = 0$).

2. **Mandel–Kelvin (MK) formalism isomorphism**: The elasticity tensors are subsequently vectorized into 3×3 MK matrices, as detailed in the *Methods* and *Supplementary Materials*. Unlike Voigt notation, the MK formalism constitutes an exact mathematical isomorphism of 4^{th}-order tensors. A fundamental property of this isomorphism is that it yields self-adjoint rotation operators, the Bond matrix. Arbitrary spatial rotations applied to the material translate into rigorous orthogonal transformations of the MK matrix, greatly facilitating consistent manipulations via direct Jacobian operators. Consequently, the eigenvalues of the 3×3 MK matrix are absolutely invariant under spatial rotations. They represent the fundamental Kelvin moduli of the material.

Because the corresponding MK matrices are strictly block-diagonal, performing an eigendecomposition naturally isolates two decoupled physical modes, yielding three strictly invariant Kelvin moduli: the two eigenvalues of the upper-left 2×2 block (λ_1 and λ_2), and the isolated $(3, 3)$ component (λ_3). The vertical axis (the trace) represents the sum $\lambda_1 + \lambda_2 + \lambda_3 = C_{11} + C_{22} + 2C_{66}$, which equates to the true invariant tensor trace. We have therefore verified that every axis represented in the multidimensional space is independent of the coordinate system.

Regarding the specific choice of anisotropy metric over the Zener ratio: the upper-left 2×2 block inherently encapsulates the coupled X and Y normal responses (combining the C_{11}, C_{22}, and C_{12} MK components). Its two invariant eigenvalues, λ_1 and λ_2, physically represent the principal bulk stiffnesses of the metamaterial. The ratio λ_1/λ_2 (plotted on the *Principal stiffness anisotropy* axis) provides an exact and invariant measure of the fundamental normal anisotropy. In the context of our highly compliant, structurally programmable metamaterials, this eigenvalue ratio is strategically more relevant than the classical Zener ratio, which is primarily designed to assess the shear anisotropy of stiffer, cubic crystal systems.

Reporting the maximum and minimum values for shear stiffness

We thank the reviewer for this request, which brought to our attention a numerical inconsistency in our initial submission. While the extraction of the C_{66} values from finite element simulations was correct, we had omitted the necessary factor of 2 when mapping the shear stiffness values in the *Supplementary Materials*, leading to a discrepancy between the reported supplementary data and the invariant eigenvalues discussed in Figure 3. The relevant supplementary figures have now been corrected.

To rigorously establish the invariant significance of this metric, it is essential to trace its mathematical definition starting from the engineering shear behavior. The physical shear stress σ_{12} is conventionally related to the engineering shear strain γ_{12} by the classical shear modulus G_{12}, denoted C_{66} in Voigt notation, via $\sigma_{12} = C_{66}\gamma_{12} = 2C_{66}\epsilon_{12}$, where ϵ_{12} is the tensorial shear strain component. However, the MK isomorphic vectorization defines the strain state vector as $\underline{\boldsymbol{\epsilon}} = [\epsilon_{11}, \epsilon_{22}, \sqrt{2}\epsilon_{12}]^{\text{T}}$. To strictly preserve the strain energy density, a condition for the self-adjointness of the Bond matrix, the constitutive relation on the third axis imposes

$\sqrt{2}\sigma_{12} = \underline{\underline{\mathbf{C}}}_{\mathrm{MK}}^{(3,3)}(\sqrt{2}\epsilon_{12})$. Substituting the conventional relation $\sigma_{12} = 2C_{66}\epsilon_{12}$ directly yields $\underline{\underline{\mathbf{C}}}_{\mathrm{MK}}^{(3,3)} = 2C_{66}$.

Because this $(3, 3)$ component is completely decoupled from the normal modes when evaluated in the principal axes, it corresponds exactly to the third invariant eigenvalue of the elasticity tensor: $\lambda_3 = 2C_{66}$. It therefore defines the absolute, orientation-independent extremal shear capacity of the material, plotted on the *Shear modulus* axis. As requested, we further confirm that our morphogenetic metamaterials cover an invariant shear stiffness range of $\lambda_3 \in [0.47, 2.22]$ GPa.

We acknowledge that this rigorous MK-based framework could have been perceived as a standard matrix plot. To prevent any ambiguity for the reader, we have thoroughly clarified in the *Results* and *Methods* sections of the revised manuscript that the reported anisotropy, shear, and trace metrics correspond directly to the invariant eigenvalues (Kelvin moduli) of the orthotropic elasticity tensors.

Modifications made to the manuscript:

- Colorbars and explicit legends specifying displacement field magnitudes have been added to panels (a), (b), and (c) of Figure 3 in the revised manuscript.
- **Main Text (Results Section, Fig. 3e discussion):** A paragraph has been added after the parametric space description to explicitly define all three axes of Figure 3e as eigenvalue-based invariants of the Mandel–Kelvin stiffness matrix: stiffness trace $\lambda_1 + \lambda_2 + \lambda_3 \in [2.31,\ 7.95]$ GPa, principal stiffness anisotropy $\lambda_1/\lambda_2 \in [1.93,\ 5.72]$, and shear eigenvalue $\lambda_3 \in [0.47,\ 2.24]$ GPa.
- **Supplementary Materials (Database Equivalence Section):** Include a paragraph detailing the derivation of the isolated pure shear mode, explicitly detailing the factor of 2 ensuring the energy-preserving transition from the engineering shear strain γ_{12} to C_{66} and ultimately to the MK eigenvalue λ_3.
- **Supplementary Materials (Equivalence of Tension... Section):** Explicitly detail the bounding values [min, max] for all explored tensor metrics, Trace, Anisotropy, and Shear λ_3, directly in the text describing the updated parameter space mappings in Figures S10 and S11.

7. Figures 5 and 6: Figures 5 and 6: Since displacement measurements are inherently dependent on the choice of a reference point, it is preferable to present these results as strain to ensure objectivity and frame-indifference.

We thank the reviewer for this relevant observation. We fully agree that representing the mechanical response through strain profiles ensures objectivity and structural frame-indifference. In accordance with your recommendation, we have computed the experimental strain tensor components (ε_{xx}, ε_{yy}, and ε_{xy}) by spatial derivation of the measured displacement fields for our three configurations. These strain maps have been added to the revised *Supplementary Materials* and are also reproduced below for your convenience.

While we recognize the theoretical superiority of this frame-indifferent representation, we have made the deliberate choice to retain the displacement fields as the primary performance metric in the main manuscript (Figures 5 and 6). This decision is motivated by two key considerations:

1. **Consistency with existing literature:** The established scientific corpus evaluating mechanical cloaking performance is overwhelmingly based on the comparative analysis of displacement fields. Retaining this formulation in the main text is therefore crucial to ensure direct comparability with previously published benchmark studies.

2. **Sensitivity to scale and local effects:** Strain fields, being computed through spatial derivation, are inherently highly sensitive to local topological features. For highly porous and structurally complex architectures such as our morphogenetic metamaterials, the global cloaking trend can easily be overshadowed by local strain concentrations or boundary effects. While the underlying displacements remain continuous and relatively smooth, the derived strain maps exhibit localized singularities. To maintain an interpretable visualization emphasizing the macroscopic performance, the presented strain color-scales have been saturated outside the $[1\%, 99\%]$ percentile range.

Despite these visualization challenges tied to the porous nature of the structure, the derived strain components clearly corroborate the recovery of the global unperturbed fields induced by the morphogenetic cloak. We trust that the reviewer will appreciate our strategy of incorporating these rigorous strain maps into the supplementary information, thereby enriching the mechanical validity of our study while preserving narrative continuity with the established conventions of the cloaking literature.

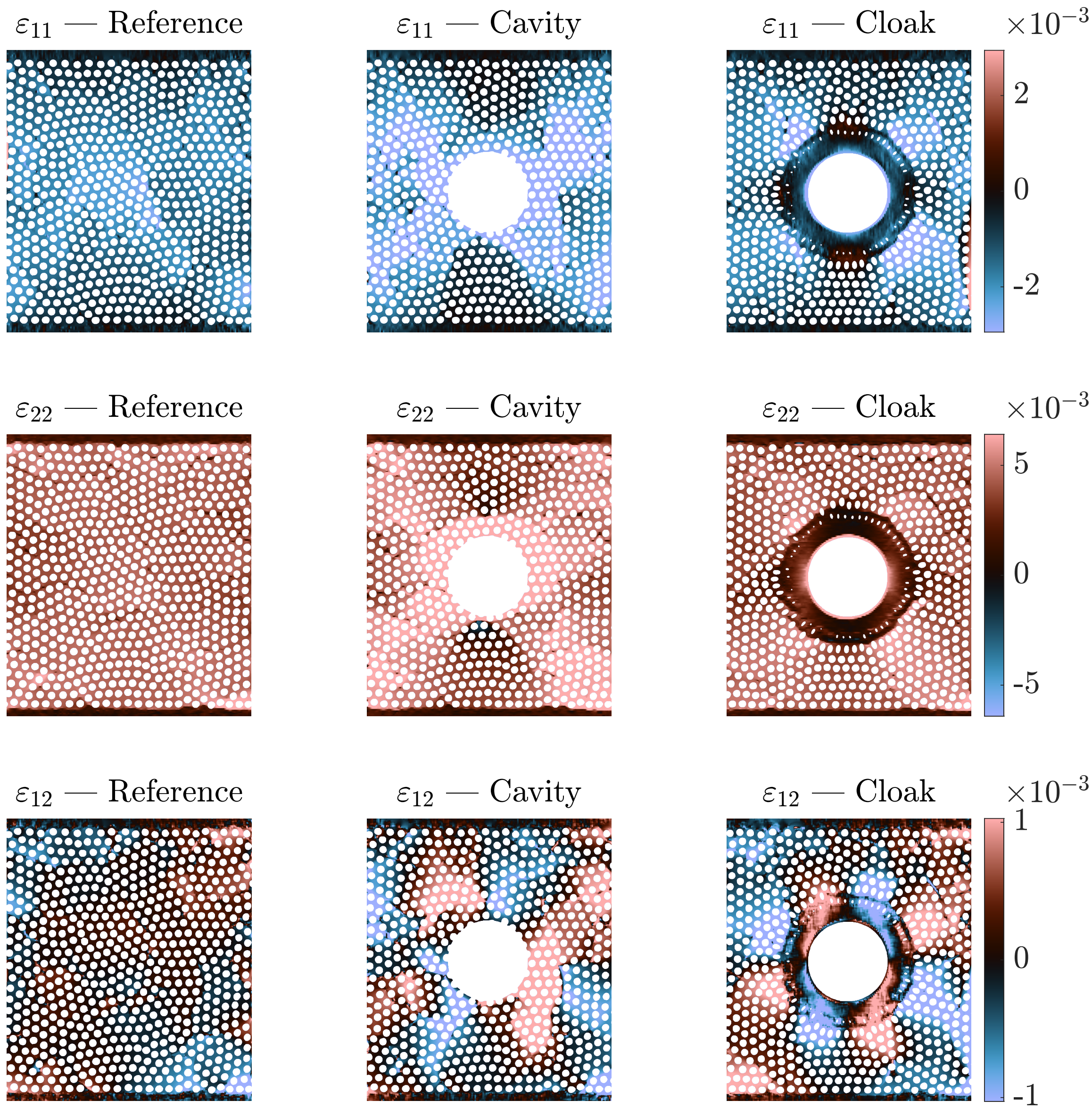

Figure C1: **Experimental strain fields.** Spatial distribution of the strain components (ε_{xx}, ε_{yy}, and ε_{xy}) obtained by spatial derivation of the experimental displacement fields. The fields correspond to the reference, uncloaked, and morphogenetic cloaked structures. Color scales are saturated to the $[1\%, 99\%]$ range to filter out local structural singularities while revealing the macroscopic behavior.

Modifications made to the manuscript:

- **Supplementary Materials:** Add the relative figure presenting the experimental strain tensor components, along with a dedicated paragraph discussing the calculation through spatial derivation, the colorbar saturation strategy, and the confirmation of the cloaking behavior. Specify the choice of the *managua* colormap (Crameri), selected for its color-blind compatibility and its sequential dynamics better suited to sign-constrained normal strain components (ε_{xx}, ε_{yy}), in contrast to the diverging *roma* colormap used for displacement fields.

8. Optimization Formulation: A formal optimization problem must be explicitly defined for any study concerning optimal design. The authors should clearly specify the target values and the optimization problem employed to minimize the deviation from these targets.

We thank the reviewer for this comment, which allows us to clarify a central aspect of our contribution. We understand the expectation that a formal optimization problem should be stated; however, proposing an alternative to this classical formulation is precisely the core objective of this work. The two diagrams below summarize the fundamental distinction between the classical optimization paradigm and our morphogenetic approach:

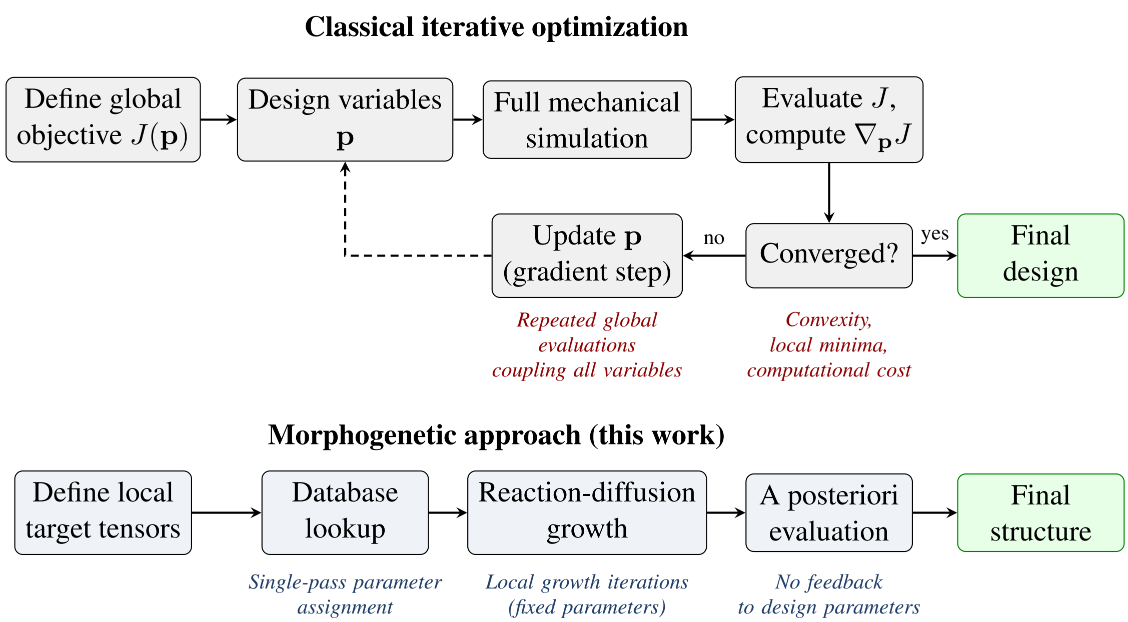

In the classical framework, the design loop couples a global objective $J(\mathbf{p})$ to iterative mechanical evaluations: at each step, a full simulation computes J and its gradient $\nabla_{\mathbf{p}} J$, and design variables are updated until convergence. This cycle is mathematically rigorous but couples all variables through global equilibrium, raises convexity concerns, and incurs costs that scale with model complexity.

Our approach replaces this loop by a forward pass. The mechanical target is encoded upstream as a field of local tensor prescriptions, converted into morphogenetic parameters through a single database lookup. The reaction-diffusion engine then iterates internally, approximately 80 000 explicit Euler steps, but these iterations serve exclusively to let the structure self-organize under fixed parameters. At no stage are the achieved mechanical properties evaluated, nor are the generative parameters modified in response to any performance assessment. Performance is assessed only a posteriori. This fundamental decoupling between design specification and structural emergence is what enables the scalability and computational efficiency of the method.

Target specification for each design strategy

The manuscript presents two complementary strategies, each with a clearly defined mechanical target. We detail below how targets are specified, the gap between objectives and achievable properties, and the resulting performance.

Transformation-based mechanical cloaking. The mechanical target for cloaking is a spatially varying field of elasticity tensors $\underline{\underline{\mathbf{C}}}'(x, y)$, derived analytically from a coordinate transformation. Starting from a homogeneous orthotropic medium $\underline{\underline{\mathbf{C}}}$, the transformation prescribes the local stiffness required to redirect stress trajectories around a cavity:

$$\underline{\underline{\mathbf{C}}}' = \frac{1}{\det(\underline{\underline{\mathbf{A}}})}\,\underline{\underline{\mathbf{T}}}(\underline{\underline{\mathbf{A}}})\,\underline{\underline{\mathbf{C}}}\,\underline{\underline{\mathbf{T}}}(\underline{\underline{\mathbf{A}}})^T,$$

where $\underline{\underline{\mathbf{A}}} = \underline{\underline{\mathbf{J}}}^{-1}$ is the inverse Jacobian of the spatial mapping and $\underline{\underline{\mathbf{T}}}$ its Mandel–Kelvin counterpart. This target field is then confronted to the finite space of achievable properties within our morphogenetic database. As detailed in the Supplementary Materials (section "Transformational Objectives and Synthesized Material Properties"), a gap inevitably exists between the theoretical targets and the synthesized properties, particularly near the inner radius R_1 where the transformation demands extreme stiffness values that exceed the physical bounds of the constituent material (0% porosity limit). The morphogenetic parameters (λ, s, θ) at each point are selected through a single-pass nearest-neighbor search minimizing the weighted distance:

$$E = w_{\text{tr}}\,|\log \text{tr}' - \log \text{tr}| + w_\theta\,|\theta' - \theta|\,.$$

No mechanical simulation intervenes during this assignment. Cloaking performance is assessed only a posteriori through the relative displacement error Δ defined in the manuscript, yielding $\Delta_{\text{cloak}} = 10.7\%$ down from $\Delta_{\text{hole}} = 39.2\%$, a $3.66\times$ improvement consistent with numerical predictions ($3.89\times$). Despite the acknowledged gap between targets and achievable properties, this performance is competitive with the data-driven optimized design of Wang et al. (Table 1 of the manuscript), while relying on a considerably simpler generative process. A natural pathway to improve this performance is to enrich the morphogenetic pattern space with forms offering greater independent control over stiffness, anisotropy, and shear behavior, thereby reducing the mismatch between target and synthesized tensor fields while preserving the decentralized character of the approach.

Stress-guided morphogenetic growth. For the structural optimization application, the objective is the reduction of the deformation energy $E_{\text{def}} = \frac{1}{2}\int \underline{\underline{\boldsymbol{\sigma}}} : \underline{\underline{\boldsymbol{\varepsilon}}}\, dV$ under a given load. A single preliminary simulation of a homogeneous domain extracts the stress tensor field $\underline{\underline{\boldsymbol{\sigma}}}$ as a mechanical blueprint. Two levels of modulation are then applied to the morphogenetic parameters. The local density is controlled by the segmentation threshold s, mapped from the normalized stress trace:

$$s = s_{\text{void}} - (s_{\text{void}} - s_{\text{dense}}) \cdot \bar{\tau}, \quad \text{with } \bar{\tau} \propto \text{tr}(\underline{\underline{\boldsymbol{\sigma}}}),$$

densifying the structure where stresses are highest. The anisotropy is controlled by aligning the diffusion tensor $\underline{\underline{\mathbf{D}}}$ with the principal stress directions and scaling its eigenvalue ratio λ by the local stress directionality. The reaction-diffusion engine then grows the structure in seconds, achieving energy reductions of up to 25% relative to a uniform baseline at identical fill fraction ($V_f = 80\%$), without re-evaluating the mechanical equilibrium during the process. Here again, the performance is bounded by the limited expressiveness of the current elliptical pattern space; enriching the generative model with more diverse morphologies would allow finer stress-aligned microstructures and further energy gains.

We recognize that this paradigm does not guarantee strict mathematical optimality, and this is a distinction we accept. This work constitutes a first proof of principle showing that decentralized self-organization, guided by calibrated local prescriptions, can produce functional mechanical structures for two distinct classes of problems. The observed gap between target and synthesized properties is primarily attributable to the limited morphogenetic diversity currently available (elliptical inclusions with coupled stiffness and anisotropy control). Enriching this generative parameter space, through richer reaction-diffusion chemistries, multi-scale patterns, or hybrid approaches combining morphogenetic growth with lightweight calibration steps, would progressively close this gap while preserving the decentralized, scalable character of the method.

Modifications made to the manuscript:

- **Main Text (Discussion Section):** Add a paragraph clarifying our departure from classical optimization formulations. We will explicitly state that our morphogenetic approach is designed as a scalable and autonomous alternative to centralized optimization methods, circumventing the need for iterative global evaluations of mechanical performance during the generative process.

2 Reviewer #2

The authors have submitted an extensively revised draft with significant improvements, particularly regarding the applicability to different load cases and the organization of the manuscript. However, I still have concerns to be addressed before I can recommend acceptance.

1. Figure 1 consists of two zoomed-in architecture images that are not particularly helpful or illustrative of what a mechanical cloak is, how it works, or what previous approaches have been tried. For such a broad/interdisciplinary journal, figure 1 should offer an overview of the paper's aim and general concepts, as well as illustrate any terms necessary to understand the paper (e.g. mechanical cloak). This figure still needs to be reworked and better integrated with the Introduction.

We thank the reviewer for this constructive feedback. We fully agree that a broader, more conceptual introductory figure is essential for a multidisciplinary journal like Nature Communications to immediately convey the core concepts of mechanical cloaking and our morphogenetic approach to the general readership.

Accordingly, we have entirely redesigned Figure 1 to provide a comprehensive structural overview of the mechanical cloaking problem and the state-of-the-art structural strategies. The revised figure now introduces the general principle of a mechanical cloak across different scales. First, Panel A presents the target macroscopic elasticity field required to redirect stress trajectories around the central cavity. The spatial variation of the continuous solid stiffness is visualized through the trace of the $\underline{\underline{\mathbf{C}}}$ tensor, mapping the local rigidity requirements.

To bridge the gap between this theoretical mapping and physical realization, Panel B clarifies the complexity of solid continuum mechanics. By visualizing the directional Young's modulus $E(\theta)$, we highlight that implementing such transformations goes beyond mapping scalar fields. It requires defining spatial transformation operators (involving coupled rotations and scaling) on 4^{th}-order elasticity tensors. Even though $E(\theta)$ is an intuitive metric, designing structures that synthesize these complex tensorial projections remains a major challenge. We emphasize that while this metric provides an intuitive representation of the target anisotropic response, our morphogenetic synthesis is rigorously based on the 4^{th}-order elasticity tensor $\underline{\underline{\mathbf{C}}}$, which is effectively mapped onto a restricted but functional design space through the synthesis of orthotropic material classes. Panels C and D then illustrate how the scientific community has historically tackled this challenge: either by applying coordinate transformations to specific discrete lattice networks (pentamode structures), or by optimizing complex pixelated unit-cell microstructures. Our paper proposes a fundamentally different, fully decentralized approach to generate these metamaterials.

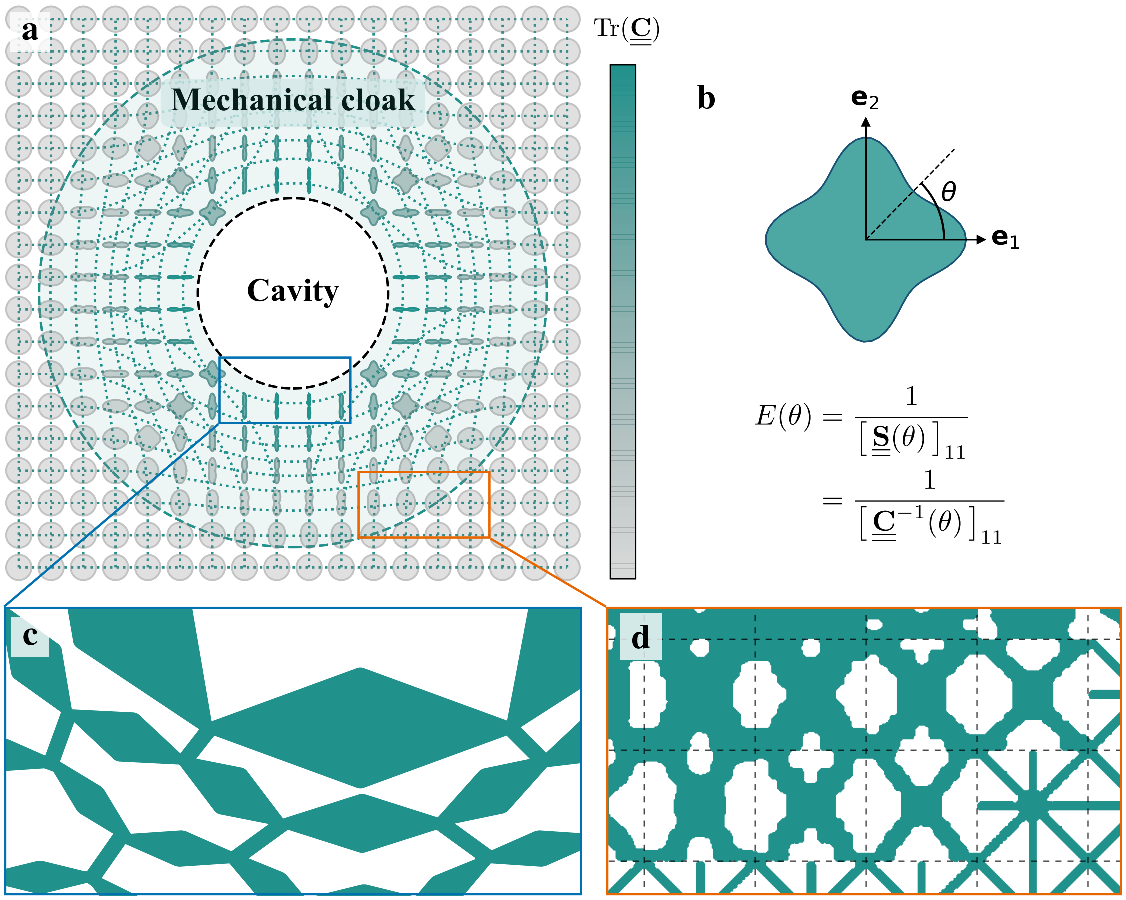

Figure C2: **Revised Figure 1.** Overview of mechanical cloaking strategies and the complexity of synthesizing effective parameter distributions.

Modifications made to the manuscript:

- **Main Text (Introduction):** Replaced Figure 1 with the newly designed conceptual overview ('Montage_Anisotropic_RD.pdf').
- **Main Text (Introduction):** Rewrote the Figure 1 caption to meticulously detail the macroscopic target elasticity field (trace of $\underline{\underline{\mathbf{C}}}$), the tensorial complexity of the directional Young's modulus projection, and the context of existing state-of-the-art lattice and unit-cell strategies.

2. The rainbow color scheme used for contour plots is not accessible to color-blind readers. Please convert figures to an accessible color scheme. (Figures throughout main manuscript and supplementary material)

We would like to thank the reviewer for raising this crucial point regarding accessibility. We fully recognize the limitations of traditional "rainbow" or "jet" color schemes, which not only lack perceptual uniformity but also represent a significant barrier for readers with color vision deficiencies.

In the revised manuscript and supplementary materials, we have systematically replaced all rainbow-type colormaps with perceptually uniform, colorblind-friendly alternatives. Specifically, we have adopted the *roma* diverging colormap (from the Crameri scientific colormap suite) to represent displacement fields, providing unambiguous visualization of positive and negative variations. Furthermore, for the newly added strain fields, we explicitly selected the sequential *managua* colormap to optimally render sign-constrained normal strain components (ε_{xx}, ε_{yy}). We believe these visually accessible color schemes greatly enhance the rigor and inclusivity of our data presentation.

Modifications made to the manuscript:

- **Main Text & Supplementary Materials (All contour plots):** All contour plots (Figures 3, 5, 6, 8, and Supplementary Figures) have been re-generated using the perceptually uniform *roma* diverging colormap and occasionally the *managua* sequential colormap.

- **Main Text (Results Section)**: A sentence acknowledging the systematic use of the accessible *roma* colormap has been added to the text.

3. Please elaborate on the description of the microstructure as "trusses" in the caption of Supplementary Fig 12.

We thank the reviewer for pointing out this terminology nuance. The term "trusses" inherently refers to a discrete structural assembly (e.g., lattice networks or articulated frameworks). Because our morphogenetic approach relies on anisotropic reaction–diffusion, it intrinsically generates a continuous porous solid medium rather than a discrete collection of beams.

We fully agree that the initial term was inconsistent with the continuum nature of our generative process. We have revised the caption of the corresponding figure (now Supplementary Figure 8) to employ a more rigorous terminology aligned with our design philosophy, highlighting the emergence of continuous material distributions rather than discrete, artificial trusses.

Modifications made to the manuscript:

- **Supplementary Materials (Section: Analysis of Stress-Field Guided Growth, Figure 8):** The caption of the displacement magnitude map (formerly Supplementary Figure 12) was rewritten from "*develops truss-like load paths*" to "*promotes a directional material distribution that aligns with the dominant stress flow*".

4. In the discussion, the authors comment that the optimization design method can be readily transferred to 3D. Please comment on the manufacturability of 3D designs.

We agree with the reviewer that stating the 3D transfer is mathematically straightforward does not account for the practical manufacturing challenges.

Indeed, a direct 3D implementation of the Turing mechanism results in closed porosity (isolated 3D inclusions). This morphology renders subtractive manufacturing impossible and severely limits standard additive techniques relying on a liquid bath or powder bed (such as stereolithography or selective laser sintering), as uncured support material becomes permanently trapped inside the structure.

To provide a more balanced perspective, we have expanded our *Discussion* to explicitly acknowledge these manufacturing limitations. While we kept the manuscript concise by simply mentioning that solutions are currently being explored, we can share with the reviewer two specific strategies currently under investigation to address this:

1. Utilizing extrusion-based additive manufacturing (e.g., FDM), which avoids the trapped-material issue entirely, potentially followed by a post-sintering step to resolve interlayer adhesion concerns.

2. Modifying the generative algorithm to mathematically enforce pore inter-connectivity (creating continuous evacuation networks), ensuring compatibility with a broader range of 3D printing technologies.

Modifications made to the manuscript:

- **Main Text (Discussion):** Inserted a short paragraph acknowledging the 3D manufacturability challenges (trapped uncured material due to closed porosity) and mentioning ongoing research into geometric and manufacturing solutions.

5. In Fig 9, please clarify what the structures/insets on the right correspond to.

We apologize for the lack of clarity in this figure.

The three insets on the right of each panel correspond to enlarged views of the three structures compared in the bar plots: the homogeneous isotropic structure (serving as reference), the graded isotropic structure (density modulation only), and the graded anisotropic structure (density and orientation modulation).

To ensure this is immediately clear to the reader, we have added explicit text labels ("Homogeneous Isotropic", "Graded Isotropic", and "Graded Anisotropic") directly next to each corresponding inset in the figure.

Modifications made to the manuscript:

- **Main Text (Figure 9):** Added text labels next to the magnified insets to explicitly identify the three types of generated microstructures.

6. For the additional loading cases added in the revised draft, the same metrics as in Table 1 should be presented to facilitate comparison between loading cases and with previous studies.

We thank the reviewer for this constructive suggestion.

To address this comment, we computed the improvement factor $R = \Delta_{\text{hole}}/\Delta_{\text{cloak}}$ for all six loading scenarios and all three growth domain resolutions (603^2, 1005^2, and 1407^2 pixels). Due to the figure and table limits of the main manuscript, we have compiled these results into a new summary table placed in the *Supplementary Materials*.

The results confirm the robustness of the generative cloaking strategy, with improvement factors ranging from $R = 2.07$ (clamped uniaxial tension, smallest domain) to $R = 8.08$ (equibiaxial tension, largest domain). Notably, the equibiaxial case exhibits the strongest cloaking performance, consistent with its axisymmetric loading symmetry. The generally increasing trend of R with resolution further supports the scalability argument developed in the Discussion.

Modifications made to the manuscript:

- **Supplementary Materials (Section: Generalization to distinct loading conditions):** Added a new table reporting the improvement factor $R = \Delta_{\text{hole}}/\Delta_{\text{cloak}}$ for all six loading configurations at three growth domain resolutions.
- **Main Text (Section: Generalization across loading scenarios and scales):** Added a sentence directing readers to the Supplementary Materials for the detailed improvement factors.

7. The presented cloaking designs seem to have a ring of (near-) solid material around the cavity. What would be the comparison between the morphogenetic designs and a plate that just added this solid ring with no other optimization?

This is an insightful observation. Indeed, the transformation-based design naturally concentrates stiffness near the cavity boundary, where the spatial mapping imposes the strongest gradients. A legitimate question is therefore whether a simple solid annular ring around the cavity, without any progressive adaptation of local anisotropy and stiffness, could achieve comparable cloaking performance.

To address this, we simulated a baseline configuration consisting of the reference porous plate with a solid annular ring of outer radius $R_2 = 2R_1$ inserted around the cavity, where R_1 is the cavity radius. This ”full cloak” has the same spatial extent as the morphogenetic cloak but involves no progressive stiffness grading or anisotropy control. We compared the relative displacement errors for four loading cases across three growth domain resolutions.

The four resulting geometries are illustrated below for growth domains of 603^2 and 1407^2 pixels:

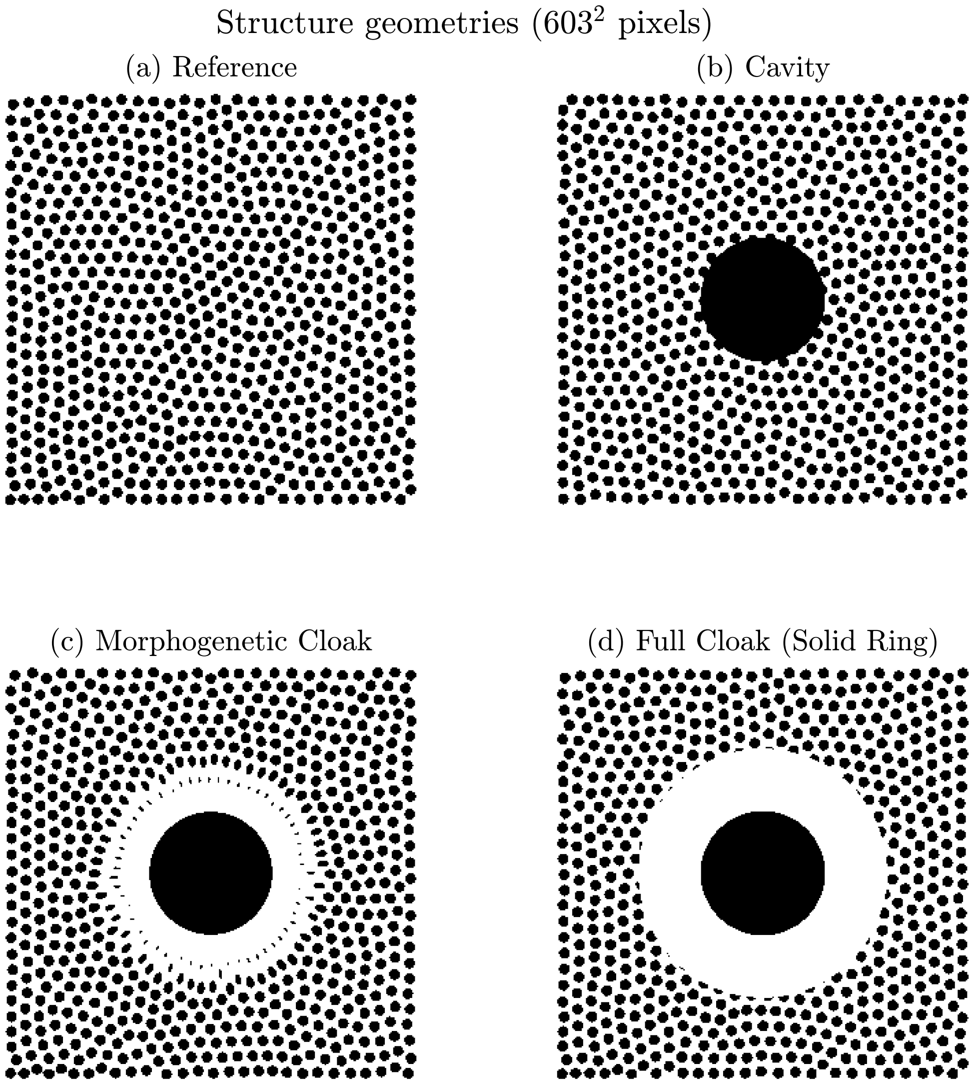

Figure C3: Comparison of the four structure geometries for growth domains of 603^2 pixels (top) and 1407^2 pixels (bottom). (a) Reference plate, (b) plate with cavity, (c) morphogenetic cloak, (d) full solid ring cloak.

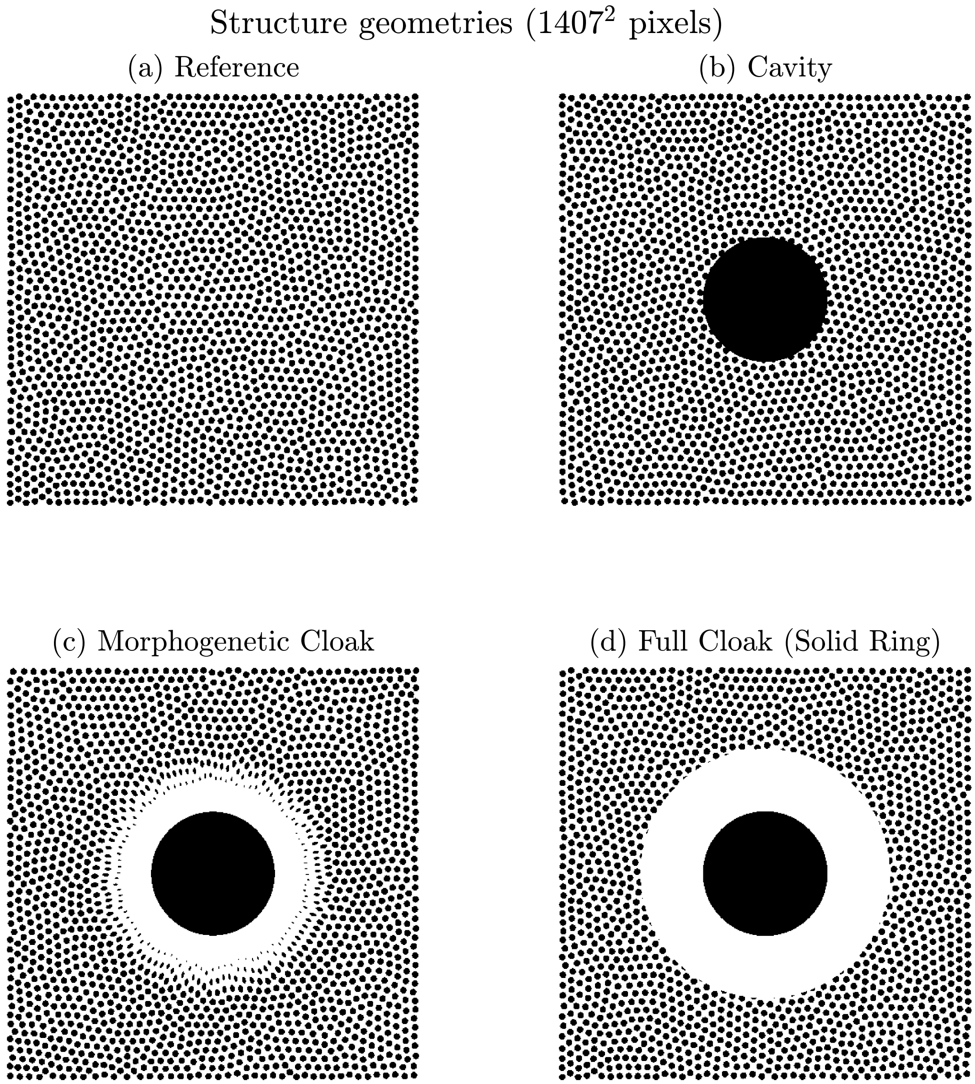

Figure C4: Comparison of the four structure geometries for growth domains of 603^2 pixels (top) and 1407^2 pixels (bottom). (a) Reference plate, (b) plate with cavity, (c) morphogenetic cloak, (d) full solid ring cloak.

The corresponding displacement error metrics are summarized below:

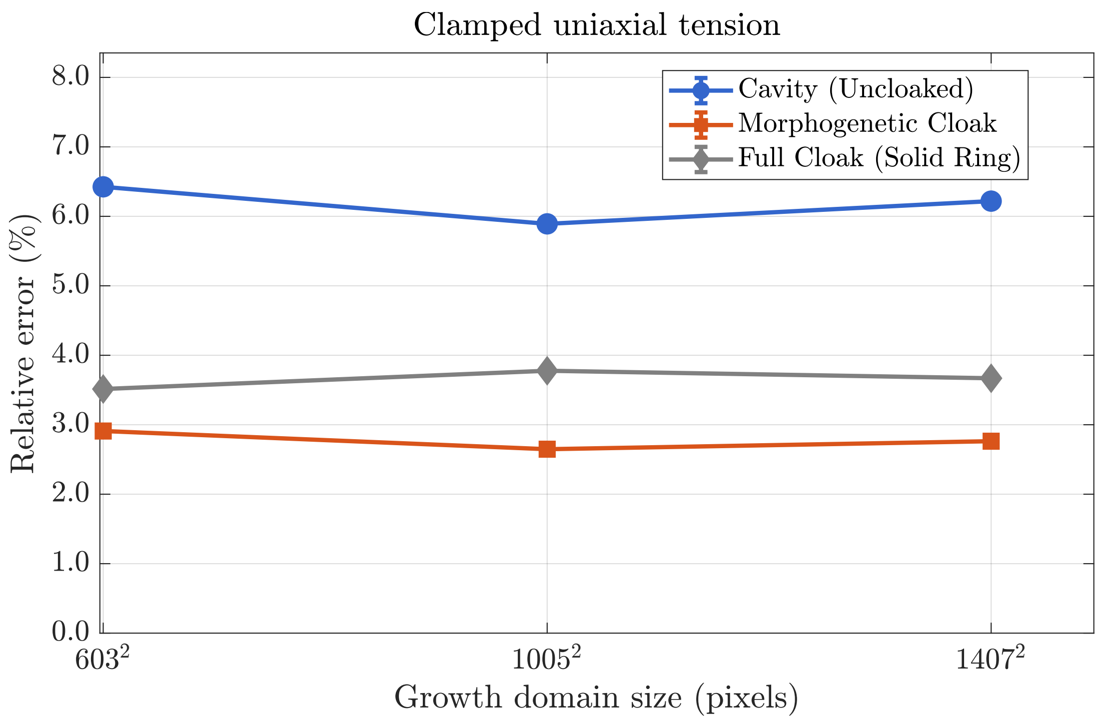

Clamped uniaxial tension
Relative error (%)
8.0
7.0
6.0
5.0
4.0
3.0
2.0
1.0
0.0
603²
1005²
1407²
Growth domain size (pixels)
Cavity (Uncloaked)
Morphogenetic Cloak
Full Cloak (Solid Ring)

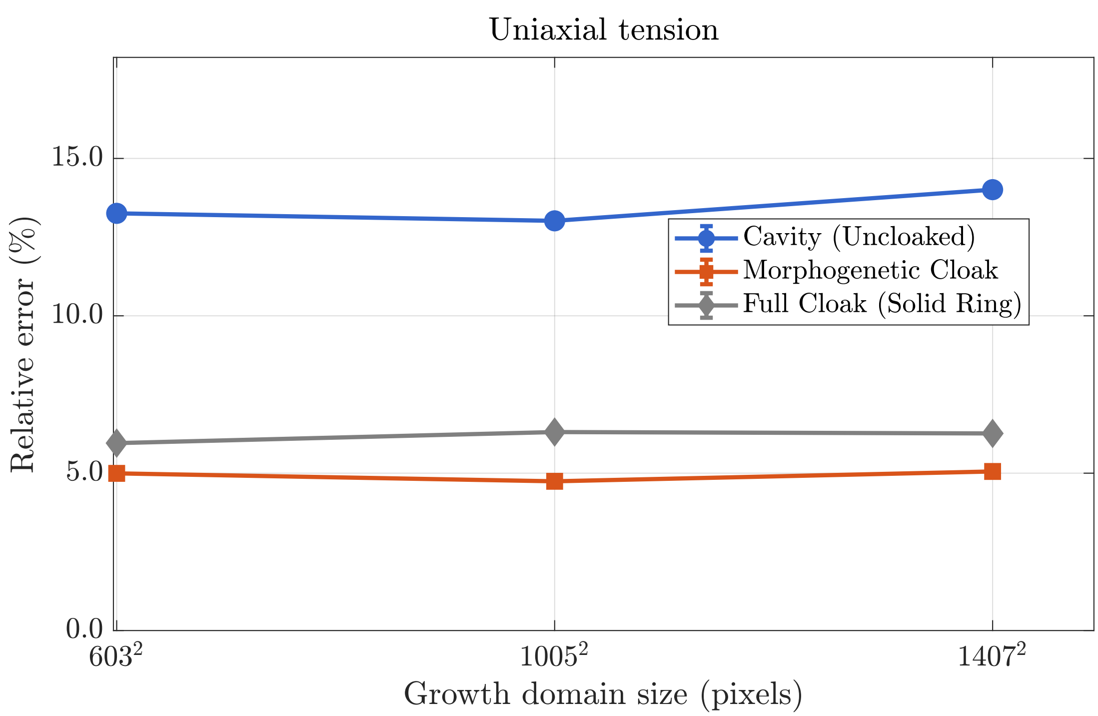

Uniaxial tension
Relative error (%)
15.0
10.0
5.0
0.0
603²
1005²
1407²
Growth domain size (pixels)
Cavity (Uncloaked)
Morphogenetic Cloak
Full Cloak (Solid Ring)

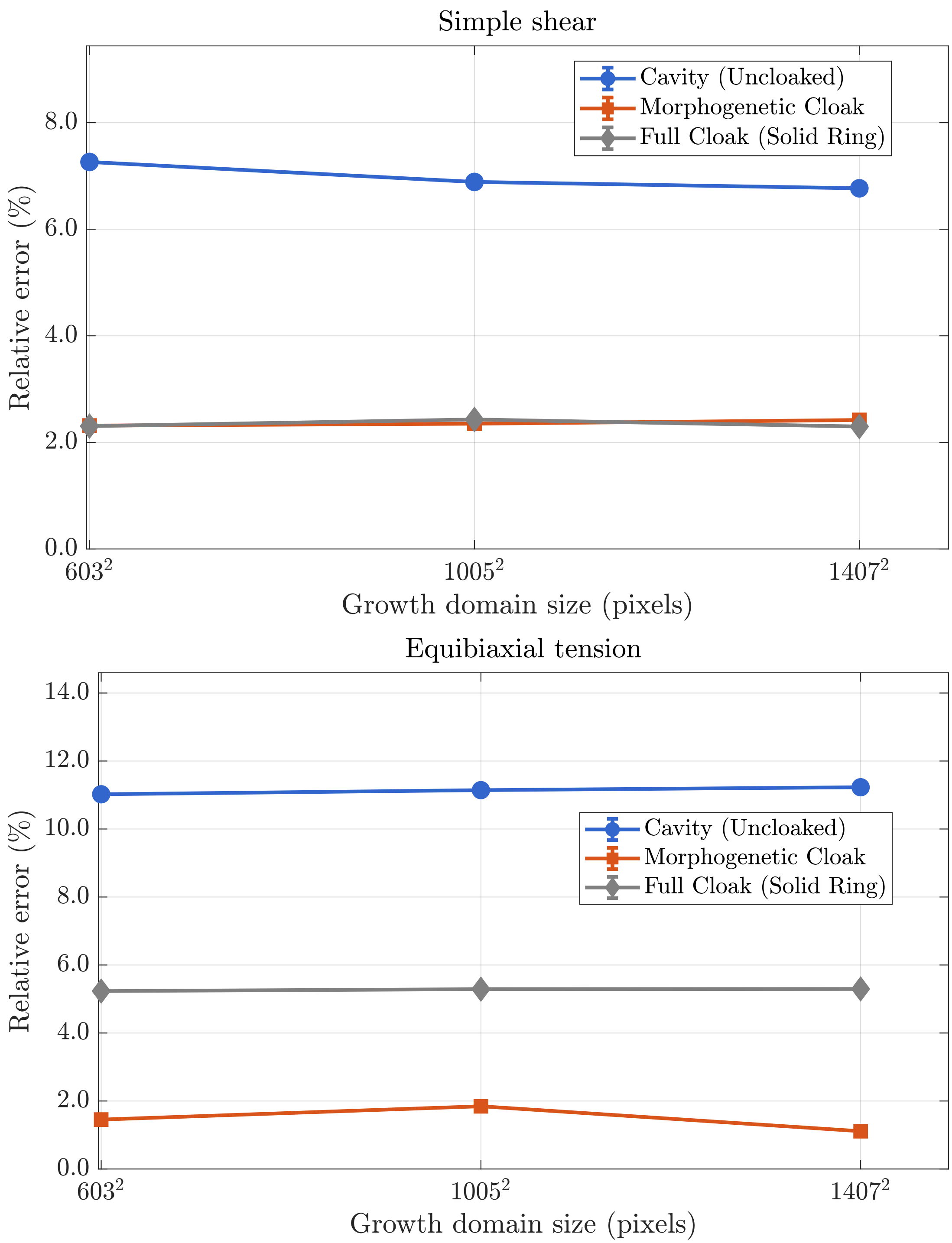

Figure C5: Comparison of the relative displacement error for three cloaking strategies: uncloaked cavity (blue), morphogenetic cloak (orange), and full solid ring cloak (gray), across four loading cases and three growth domain resolutions.

The morphogenetic cloak consistently outperforms the solid ring in three out of four loading cases:

- **Equibiaxial tension:** The morphogenetic cloak achieves improvement factors of $R = 6.0$–10.1, compared to only $R \approx 2.1$ for the solid ring (a performance ratio of approximately $3\times$ to $5\times$ in favor of the morphogenetic design).
- **Uniaxial tension:** $R_{\text{morpho}} = 2.7$–2.8 versus $R_{\text{full}} = 2.1$–2.2.
- **Clamped uniaxial tension:** $R_{\text{morpho}} = 2.2$–2.3 versus $R_{\text{full}} = 1.6$–1.8.

For **simple shear**, both approaches yield comparable improvement factors ($R \approx 2.8$–3.1). This is expected: the current generative mapping controls local stiffness and tensile/compressive anisotropy but does not explicitly target shear stiffness, as the parametric reduction from the full fourth-order elasticity tensor to the morphogenetic parameters involves a scaling on the stiffness magnitude and the principal anisotropy ratio. Extending the generative model to shapes more complex than ellipses, with additional geometric degrees of freedom, would open the possibility of explicit shear stiffness control and further differentiation from simpler baselines.

These improvements are achieved with a **lower** fill fraction. The morphogenetic cloak structures have an average fill rate of approximately 61.6%, compared to 64.9% for the solid ring configuration. These results highlight that local stiffness plays a central role in the cloaking mechanism, which is consistent with the saturation of the generative process near the cavity and the emergence of a near-solid core in the morphogenetic designs. However, the progressive adaptation of stiffness and the local control of anisotropy also play an important role in optimizing the cloaking function, as evidenced by the systematic improvement of the morphogenetic cloak over the solid ring in most loading cases. This observation is in good agreement with the results obtained through the stress-guided growth strategy presented in the manuscript, where enabling anisotropy control consistently yields further reductions in strain energy compared to density modulation alone.

Modifications made to the manuscript:

- The comparison is provided in this response as additional evidence supporting the effectiveness of the morphogenetic approach.

3 Reviewer #3

Thank you for providing additional examples of the algorithm and expanding the analysis. I recommend the paper for publication.

We are grateful to the reviewer for their recommendation and for the significant time and effort they have invested in the evaluation of our manuscript.

4 Conclusion

In conclusion, we thank all reviewers for their thorough evaluation. We hope the evidence presented here effectively confirms the potential of this new morphogenetic synthesis method for mechanical metamaterials. Rather than competing with centralized optimization, our approach draws inspiration from biological systems where complex structures and functions emerge without global computations. This decentralized path offers a versatile and practical design strategy where scalability is inherently guaranteed, with algorithmic complexity scaling linearly with the domain size thanks to purely local calculations. We believe this paradigm opens a new and efficient route for the scalable design of functional mechanical metamaterials.

Sincerely,
Thomas Fromentèze, on behalf of all authors

Morphogenetic mechanical metamaterials

Emerging tensor properties from self-organized structures

Response to Final Editorial Review

Thomas Fromentèze,[1,2,*] **Philippe Michaud,**[3]
Ali Hassny,[4] **and Vincent Pateloup**[3]

[1] University of Limoges, CNRS, XLIM, UMR 7252, F-87000 Limoges, France

[2] Institut Universitaire de France (IUF)

[3] University of Limoges, CNRS, IRCER, UMR 7315 , F-87000 Limoges, France

[4] University of Limoges, IUT du Limousin, F-87000 Limoges, France

[*] Corresponding author: thomas.fromenteze@unilim.fr

Dear Reviewers,

We thank the reviewers for their satisfaction with our revisions. Their feedback throughout the review process has helped us clarify and strengthen both the presentation and the scientific content of our work.

Below, we provide a point-by-point response to the remaining comments, detailing the clarifications and modifications we have made to address all outstanding points.

1 Reviewer #1

The authors have adequately addressed all outstanding points from the previous round of review. The reviewer is pleased to recommend the manuscript for publication in its current form.

We thank Reviewer #1 for their positive assessment and their recommendation for publication.

2 Reviewer #2

Thank you to the authors for their dedicated work on revising the manuscript. I have one remaining note: In the caption to Figure 1, the authors state "The objective of a mechanical cloak is to protect a central region from external static loads by smoothly routing stress trajectories around it." However, in the introduction, the authors define the objective of mechanical cloaks as being to make "the displacement and stress fields outside the cloaking region remain identical to those of a homogenized medium, effectively rendering the object invisible to mechanical probing." I would agree more with the latter definition, which distinguishes a mechanical cloak from simply adding reinforcement around a void. The authors should ensure their definitions are consistent throughout the manuscript. Otherwise, I recommend moving forward with the manuscript.

We agree with the reviewer's point on consistency. We have revised the Figure 1 caption to align with the Introduction definition, emphasizing that the objective of mechanical cloaking is to ensure displacement and stress fields outside the cloaking region remain identical to those of a homogeneous medium, thereby rendering the enclosed region mechanically invisible. This more precisely distinguishes our transformation-based approach from simple structural reinforcement. We thank the reviewer for this final request and for the recommandation to accept this work for publication.

3 Conclusion

In conclusion, we thank all reviewers for their thorough and thoughtful evaluation of our work. Their careful scrutiny has strengthened the precision and coherence of our presentation. We are confident that the manuscript now clearly articulates both the scientific objectives and the innovations of our morphogenetic approach, and we look forward to its publication in Nature Communications.

Sincerely,
Thomas Fromentèze, on behalf of all authors